5-22-2006

Designing a Method for Measuring Magnetoresistance of Nanostructures

Donald Scherer
University of New Orleans

DESIGNING A METHOD FOR MEASURING MAGNETORESISTANCE OF NANOSTRUCTURES

A Thesis

Submitted to the Graduate Faculty of the
University of New Orleans
in partial fulfillment of the
requirements for the degree of

Master of Science
in
Physics

by

Donald James Scherer II

B.S., University of New Orleans, 2003

May 2006

ACKNOWLEDGEMENTS

My road to the accomplishment of this graduate degree has been long and arduous. I would be remiss to take all of the credit for the work that I am about to present, since I have been helped in ways, both large and small, by many people throughout this process. I will attempt to thank those people here, but I already know that my mere words will not be enough to express the gratitude I have for everyone who has influenced me positively through this ordeal.

Firstly, I must thank Dr. Leszek Malkinski for his support and encouragement through these years. The assistantship and support are only a small part of the support I have received from Leszek. He has taken a recent graduate with no background in Material Science, and turned me into someone who dreams of reaching towards new and exciting magnetic material technologies. He has been supportive, helpful and understanding, even now, despite his own great loss to Hurricane Katrina. For his help, tutelage and support, I offer my unrestricted thanks.

I would also like to thank Dr. Frank Griffith for his endless hours of personal advice and encouragement through the years. I thank Dr. Jinke Tang for answering countless hours of technical questions, even when they where not related to his class of research. I thank Dr. Carl Ventrice, Dr. Leonard Spinu and Dr. Kevin Stokes for allowing me to borrow equipment, time and knowledge.

I must also thank Dr. Andriy Vogt for his interest in my projects, his help when I get stuck, and his great attitude and inspiration when I felt beaten.

Without question, great thanks are due to Ms. Sandra Merz of the Physics Department for her constant help in dealing with the seemingly endless bureaucratic paperwork throughout my education.

Most importantly, I would like to thank my wife and children for their support, encouragement and love. For my family, it is impossible to understand why some small detail is exciting or important, but through it all, they smile and feign excitement alongside of me, if only to make me feel supported. I must acknowledge that my accomplishments come at a great price of their time, effort and understanding. For that I am truly, completely and undying grateful.

TABLE OF CONTENTS

LIST OF FIGURES

ABSTRACT

The ultimate intent of this research program is to produce nano-sized magnetic tunneling junctions, and to study the physical properties of such devices. The physical phenomena of nano-sized tunneling junctions are significantly different than that of currently popular micro-sized junctions. There is a considerable amount of work that must be done prior to producing these new junctions to ensure that good measurements can be carried out once the structures have been built. This thesis describes the efforts taken to design a measurement platform that will accurately measure tunneling magnetoresistance (TMR) in nano-sized Magneto-tunneling Junctions (MTJ). The testing done with this system at various stages throughout the design and testing process confirm the expectations for the performance of the system. Voltage-current measurements can be performed on objects ranging from a few nanometers in size to micrometer sized. Traditional micro-sized MTJs have not been excluded in this design.

INTRODUCTION

1.1 Motivation

In the world of semiconductor electronics, size has been rapidly becoming more and more important. Today's requirements for miniaturization of electronics devices are forcing computer chip and storage manufacturers to engineer and build smaller and smaller devices. As the size of semiconductor devices drops into the sub-micrometer size range, the classical model of electron behavior becomes less applicable. These new devices are subject to the wavelike properties of quantum mechanics. In the view of classical semiconductor electronics, this quantum mechanical behavior is seen as disruptive and counterintuitive.

In the modern research world, the presence of quantum mechanical properties in nano-sized semiconductor devices is seen as a grand opportunity. If these devices could be designed to take advantage of the quantum properties of the electron, the gains for the electronics industry could be enormous. Instead of struggling to find a way to model these quantum mechanics effects in a classical sense, researchers are working to produce new, smaller devices that utilize the quantum information in electrons. Electron spin tunneling is one of these quantum phenomena.

Quantum mechanics teaches us that electrons have spins. This spin is closely related to magnetism. In a classical semiconductor device, this spin is not relevant. New research in the thin film materials arena has produced devices that have different physical properties depending on the spin of the electron traveling through the device. These devices are sometimes called spintronic or magneto-electronic, in reference to their spin and magnetic based properties.

I wish to develop some Magnetic Tunneling Junctions (MTJs) on the scale of a few nanometers size. These MTJs will be spin dependent. In order to properly test the structure and properties of such devices, it is necessary to create a measurement system that is

specifically designed for these devices. The effort to create that measurement system is discussed in this thesis.

1.2 Theoretical Background

(Tunneling Junctions)

Quantum Mechanics opened many new doors in the areas of both theoretical and applied science. The rapid miniaturization of computer electronics quickly changed the focus of microelectronics engineering from the classical world to the quantum world. This change can lead to many new innovations in both the computer and electronics industries.

Among the consequences of quantum mechanics is the possibility of an electron tunneling through a barrier of higher energy than the electron. This sort of transport is clearly forbidden in classical dynamics, but becomes acceptable and predictable in quantum mechanics. In the 1960's and 1970's, as quantum mechanics was becoming better understood, advances in material technology allowed for the creation of some artificial tunnel junctions to make use of this concept. These tunnel junctions were typically made up of Metal/Insulator/Metal. Other experiments were performed with some Metal/Insulator/Superconductor junctions, as well. In these junctions, tunneling of electrons across the insulating barrier was achieved using a bias voltage. This voltage, applied through electrodes across the two metal layers of the structure, caused electrons to tunnel through the insulating barrier. In addition to electron charge, the magnetic moment can be tunneled through a barrier.

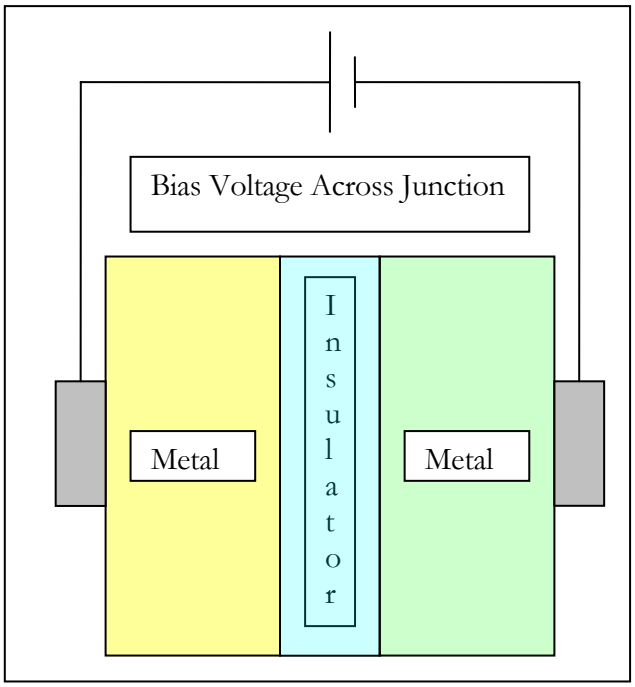

Fig. 1.1. Diagram of Early M-I-M Biased Junction

Any background research in the field of magnetic tunneling junctions brings one back to the Jullière model [1]. In 1975, Jullière created magnetic tunneling junctions using two ferromagnetic substances separated by an insulating layer. Using this type of Ferromagnet/Insulator/Ferromagnet sandwich (F-I-F), Jullière successfully measured Tunneling Magneto-Resistance (TMR). Understanding this original model is of utmost importance to the modeling of today's junctions.

Jullière's model for his MTJ was based on his assertion that the tunneling current should be influenced by the relative orientation of the magnetizations of the ferromagnetic electrodes. Jullière used ferromagnetic materials because he knew he could control the magnetic orientation in these materials through the use of an external magnetic field. Jullière's actual junctions were made with Iron and Cobalt as the

ferromagnetic ends and Germanium as the insulating layer. Jullière applied a magnetic field to the junction, aligning the magnetic orientation of the two ferromagnetic layers in a like direction. Then, by applying a magnetic field below the coercivity of one material, but above the coercivity of the other, Jullière was able to create a magnetic orientation change in just one of the ferromagnetic electrodes. Jullière reversed the magnetic orientation of just that electrode. Jullière put forward that the tunneling current would be less when the ferromagnetic electrodes' magnetic orientations were aligned antiparallel, than when they were aligned parallel. Jullière actually observed this result with his junctions.

This resistance gain due to the relative orientations of magnetization of two magnetic materials in a junction is what we refer to as TMR. To measure TMR, it is necessary to know the resistance of a tunneling junction with parallel magnetic orientations. We assign the variable $\mathbf{R_P}$ to this value. We also need to know the resistance of that same tunneling junction with anti-parallel orientation. For this we assign the variable $\mathbf{R_{AP}}$.

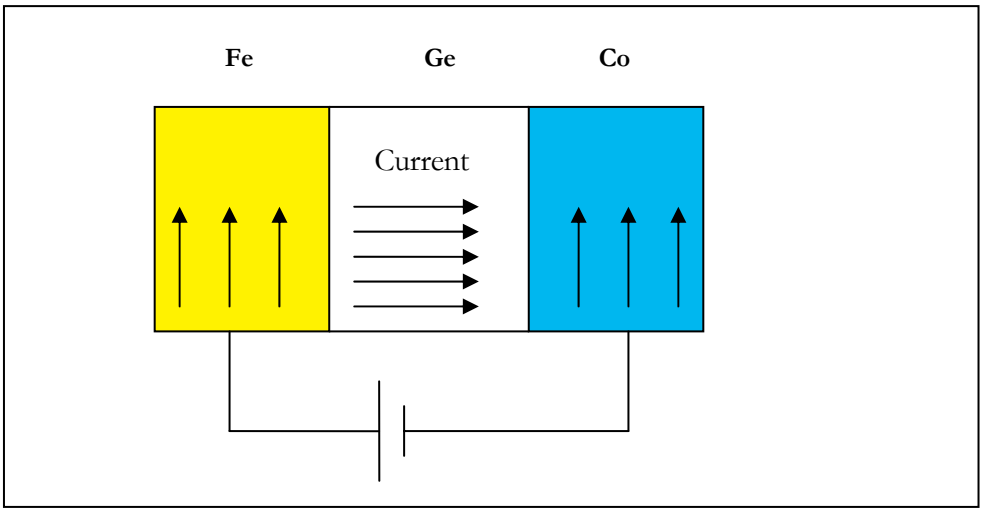

Figure 1.2 Ferromagnetic Interaction with Parallel Orientation (Jullière)

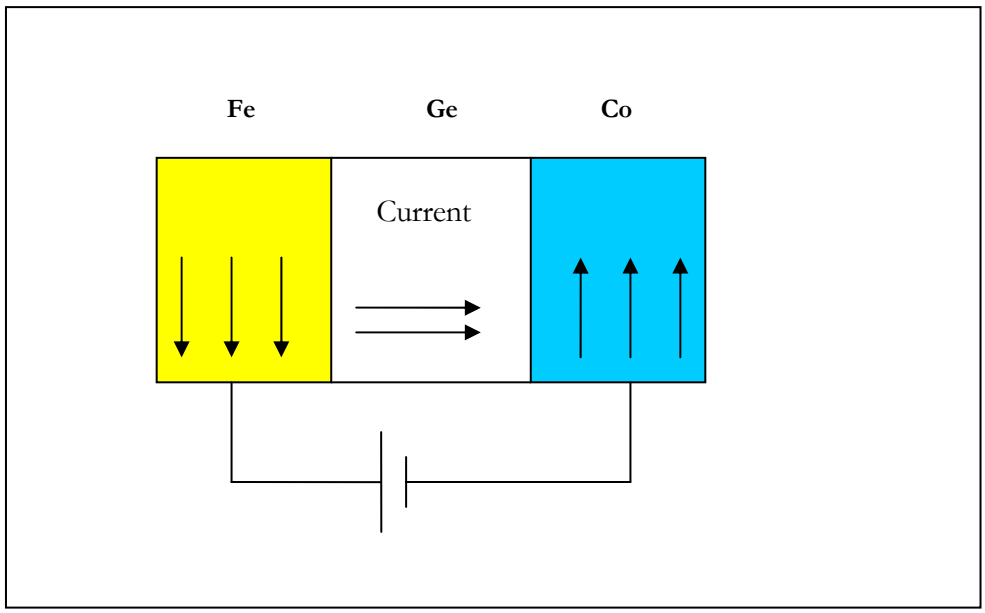

Figure 1.3. Antiferromagnetic Interaction with Anti-Parallel Orientation (Jullière)

The two figures above (1.2 and 1.3) show the results that were observed by Jullière. This representation shows the lower value of electrical current traveling through the junction. This equates to an extra resistance due to tunneling, and this is what we call TMR. The equation for TMR is generally defined as:

$$\mathbf{TMR(\%) = 100 \times (R_{AP} - R_P) / R_{AP}} \qquad \text{(eq. 1.1)}$$

Despite Jullière's success at creating a junction and finding measurements that supported his hypothesis, the field of magnetic tunneling remained at a standstill for nearly 20 years, waiting for the fabricating techniques to catch up to the physics.

In 1995, the discovery of large and reproducible TMR in room temperature settings led to a renewed interest in the research and exploitation of tunneling junctions. Years of modernization in the field of deposition techniques exposed scientists to better

material production controls. These controls allowed for the creation of better insulator layers, solving the problems that had plagued Jullière. Moodera et al. [2] built new junctions using different materials, and achieved much greater results. The junctions built by Moodera et al. were made of $Co/Al_2O_3/CoFe$. Moodera et al. reported TMR results of 18% with their junctions. Their use of alumina, Al_2O_3 , as the instulating layer, has been widely reproduced.

Today, alumina is still very common in junctions. Although alumina can be directly deposited onto metallic electrodes, the growth and the metal/insulator interface is not good. This leads to bad magneto-resistance characteristics at the interface between the metal and the insulator. In order to continue to use alumina as an insulating layer, the process is now generally performed in two steps. First, aluminum is deposited directly on the metal in a stripe measuring only a handful of Angstroms thick. Then, in a second phase, the aluminum is oxidized in place. This oxidation can be performed in different ways. The two most common methods for oxidizing the aluminum are by plasma oxidation, or by simple exposure to oxygen. Either method produces an insulating layer that adds to the effect of TMR.

These new junctions that were produced by Moodera et al. exhibited a high enough TMR value at room temperature to be useful as a new technology. The results of this experiment described a junction that had a low saturation magnetic field, and a high sensitivity to an applied magnetic field. Until this time, these devices showed these sort of TMR effects at extremely low temperatures. The ability of these specific junctions to maintain these properties at room temperature made it a good candidate for some real-world technologies. Among the first of these technologies was the junctions use as

a magnetic sensor. This also made the junction a good candidate as a magnetic read head for computer storage technology. Needless to say, once the computer companies observed an exploitable property in tunneling junctions, research funding increased, and the world of magnetic tunneling junctions reawakened after a 20 year nap.

TMR proved useful in its early days of inception, but as is common in most new technologies, "higher, faster, stronger" was the cry from researchers. As fabrication techniques continued to improve, the amount of control over layer thickness and junction size and shape rapidly advanced. As a consequence, researchers were able to build junctions using differing thicknesses of both metal and insulator layers. This allowed more experimentation to add to the theoretical work describing the function of these junctions, and just which physical factors mattered to what degree. It became quickly apparent that the thickness of the insulating layer played an integral part in the value of TMR experienced in a given junction. The reason that the insulating layer thickness is so important is that the theory of TMR depends on the spin of the electrons that are crossing the barrier, and this spin is more likely to be maintained across the barrier if the barrier is thin.

Simple F-I-F junctions have usefulness in the world of technology, other advances besides this structure were inevitable. As fabrication techniques became more and more advanced, the ability to create "sandwiches" of magnetic layers was exploited. In these sandwiches, multiple layers of ferromagnetic material are stacked with non-magnetic spacers in between. The resistance through this sandwich is directly related to the coupling of the magnetic orientations of the ferromagnetic layers. When the ferromagnetic layers are coupled ferromagnetically (with magnetic orientations

aligned), the resistance is lower than when the layers are coupled antiferromagnetically in an alternating fashion. The resistance due to antiferromagnetically coupled alternating layers is very large, and thus has taken on the name Giant Magneto-resistance (GMR). These sandwiches also depend on electron spin dynamics as the mechanism for the increased resistance in the device. However, the physical phenomenon that creates a higher resistance in GMR structures is not the same one that creates a higher resistance in MTJ structures. This GMR effect was first noticed in 1988 in Fe/Cr lattices [3]. The magneto-resistance of Fe/Cr super-lattices has been measured to exceed 100%[4].

The notable resistance change (GMR) in super-lattices of ferromagnetic materials is induced by externally applied magnetic fields, as in the case of simple tunneling junctions. This externally applied field is manipulated to change the magnetic orientation of the coupled ferromagnetic layers in the super-lattice. Since the magnetic orientation of the ferromagnetic layers is being altered, the density of states of the electrons in the layer is being altered. This density of states is not just particle based, but is based on the spin of the electrons themselves. As a consequence, the actual magneto-resistance effect that is observed in these sandwiches is also based on the spin of the electrons themselves. This coincides with the work of Jullière on his first magnetic tunneling junctions. This dependency of MTJs and super-lattices on electron spin forces electronics engineers and scientists to abandon the simple "voltage equals current times resistance" view of electronics, and instead focus on the quantum effects of spin in micro-electronics and nano-electronics.

1.3 Theoretical Background

(Spin Electronics)

As discussed in the previous section, tunneling magneto-resistance and giant magneto-resistance are both dependent on the spin of the electrons in the ferromagnetic layers. The spin acts like an intrinsic microscopic magnet carried by each electron. The general topic of studying these new effects is called spin electronics. More often, you will hear this referred to as "spintronics". To understand the functionality of spin dependent tunneling, it is important to understand the physics behind the phenomenon.

When Jullière studied tunneling through his Fe-Ge-Co junctions, he assumed he was dealing with a two current model. Jullière recognized that the current of the up-spin electrons and the current of the down-spin electrons functioned independently of one another, affected by different physical conditions in the junction. Jullière's assumption is that the electrons in his junction did not undergo a spin flip during the tunneling process, and thus the current streams remained intact throughout the tunneling process. In Jullière's model, the tunneling conductance is proportional to the spin-resolved densities of states in each ferromagnetic layer. By this, Jullière thought that the up-spin density of states (DOS) in each of the ferromagnetic layers directly affected the conductance of up-spin electron current, and the down-spin DOS had the same effect on the down-spin current. Jullière tied the value of the DOS to the tunneling conductance through calculations of the polarization in each ferromagnetic

layer. The polarization calculation for the layers includes the spin-resolved DOS in each layer of ferromagnetic material. As shown in figure 1.4 below, when the magnetic orientation of the two ferromagnetic layers is parallel, the majority spin electrons from one layer tunnel to the majority state band of the other layer. Since there is no gap in the state densities, there is no need to apply a bias to achieve energy coincidence. The bias voltage that is applied is only to accomplish tunneling across the barrier.

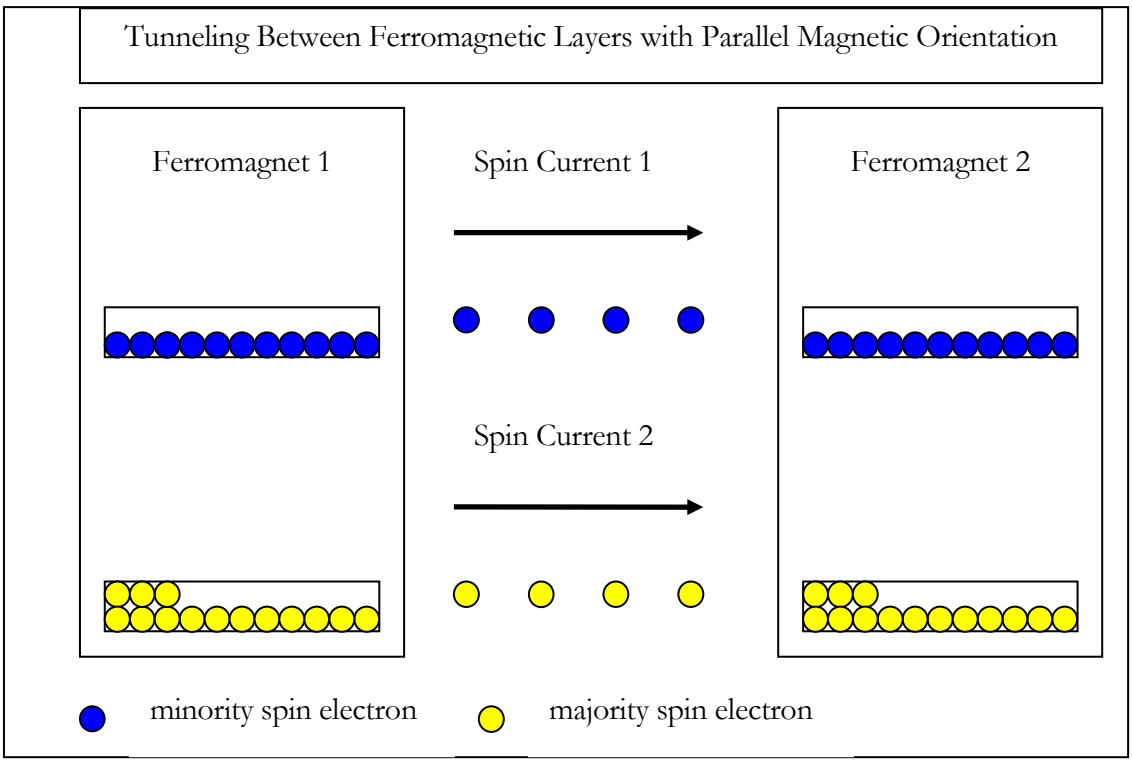

Figure 1.4 Spin Dependent Tunneling Between Ferromagnets 1

When the same layers are placed in anti-parallel magnetic orientation, we get a different set of circumstances. Figure 1.5 below shows visually how the anti-parallel magnetic orientations affect the two current streams. Here, the opposite orientation misaligns the densities of states, and forces the majority spins to tunnel to the minority band of the other layer, and vice-versa. Due to the fact that these two densities are not

at energy coincidence, there is a certain resistance to the electrons traveling between these bands. This is the effect that Jullière expected to see.

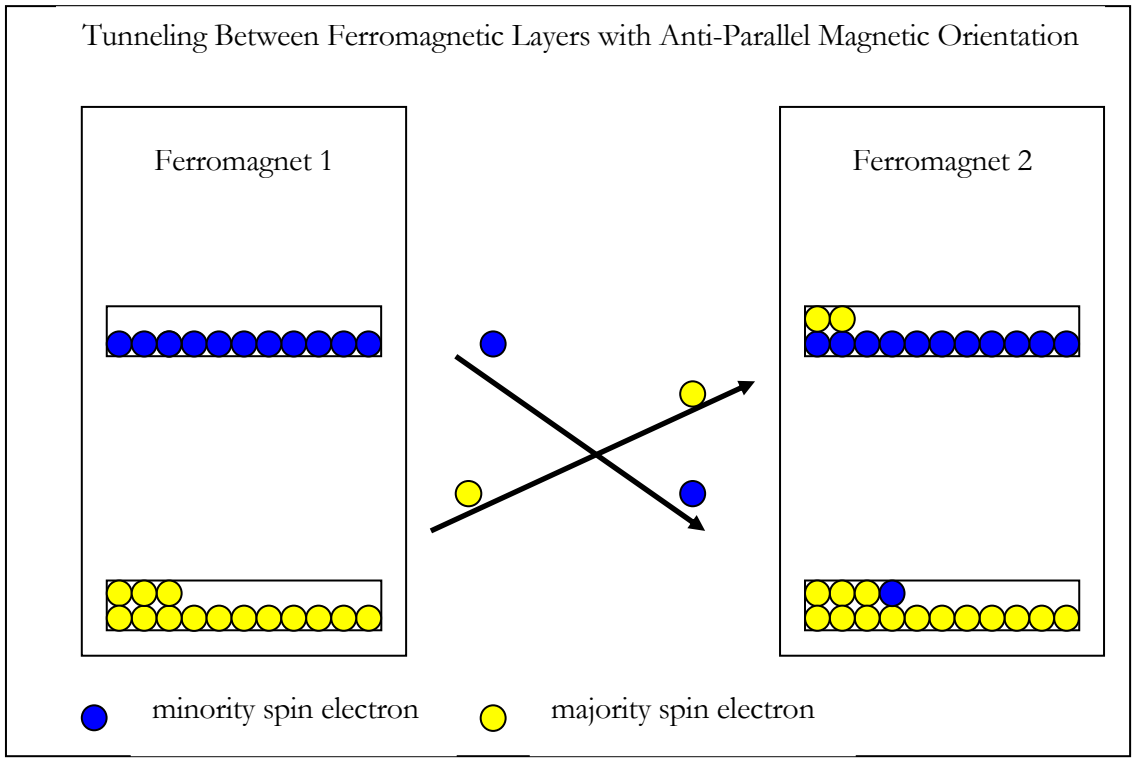

Figure 1.5 Spin Dependent Tunneling Between Ferromagnets 2

Jullière defined G_F as the conductance when the ferromagnetic layers have parallel alignment of the magnetic orientations. Similarly, he defined G_A as the conductance for the anti-parallel arrangement. Jullière calculated a value that he called the magneto-conductance ratio, $\Delta G/G$, where $\Delta G = G_F - G_A$ and G is the conductance through the junction without magnetic orientation realignment. Jullière defined this value as,

$$\frac{\Delta G}{G} = \frac{2(P_1 P_2)}{1+(P_1 P_2)} \qquad \text{(eq. 1.2)}$$

where P_1 and P_2 are the calculated polarizations of the two ferromagnetic layers.

Jullière measured a magneto-conductance ratio of 14% in his junctions, held at 4.2 K. In light of current calculations for the polarization of Fe and Co, this figure is low. As stated before, the polarization of the materials is generated from the density of states in the material. Specifically,

$$\mathbf{P = (n^{\uparrow} - n^{\downarrow}) / (n^{\uparrow} + n^{\downarrow})} \quad \text{(eq. 1.3)}$$

where $\mathbf{n}^{\uparrow}$ is the number of spin-up valence electrons in the material, and $\mathbf{n}^{\downarrow}$ is the number of spin-down valence electrons. Regardless, Jullière's charge that the difference in the conductance was based on the spin-dependent current channels has come to be accepted in modern magneto-electronic engineering.

A similar condition exists for the giant magneto-resistance (GMR) effect. GMR is not completely understood, but the effect can be modeled using the two-current model put forth by Jullière. With a GMR super-lattice structure similar to the one discussed earlier, the resistance can be considered by considering the scattering that a conduction electron might encounter. Sticking to the two-current model, a conduction electron is most likely to scatter when it encounters a scattering site with the opposite spin. Thus, if we consider the GMR super-lattice with anti-ferromagnetic coupling, we can clearly see that the electrons of either up or down spin regularly encounter scattering sites of the opposite spin. These anti-parallel spin interactions create a strong influence on the scattering of the conduction electron. Also, these electrons encounter some weak scattering influence from the layers with parallel magnetic orientation, though this term is greatly overwhelmed by the anti-parallel spin interaction. These anti-parallel scattering sites shorten the mean free path of these electrons, creating a

current channel based resistance through the super-lattice. This phenomenon is represented in Figure 1.6 below.

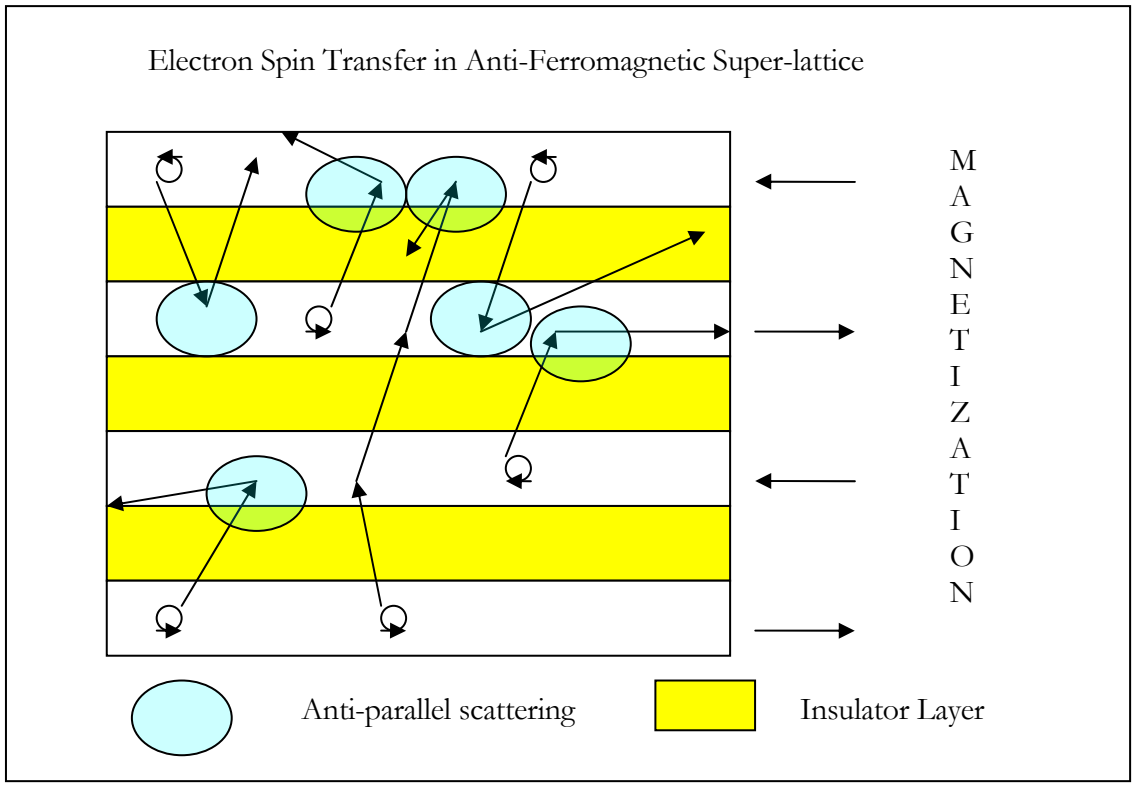

Figure 1.6 Anti-Ferromagnetic Super-Lattice GMR Scattering

On the other hand, when the same structure is induced into ferromagnetic coupling, only the electrons with opposite spin alignment to the magnetic orientation encounter any kind of strong scattering influence. The majority of the conduction electrons will encounter only weak parallel spin scattering influences, and the resistance through the super-lattice decreases dramatically. This decreased scattering can be seen in figure 1.7 below.

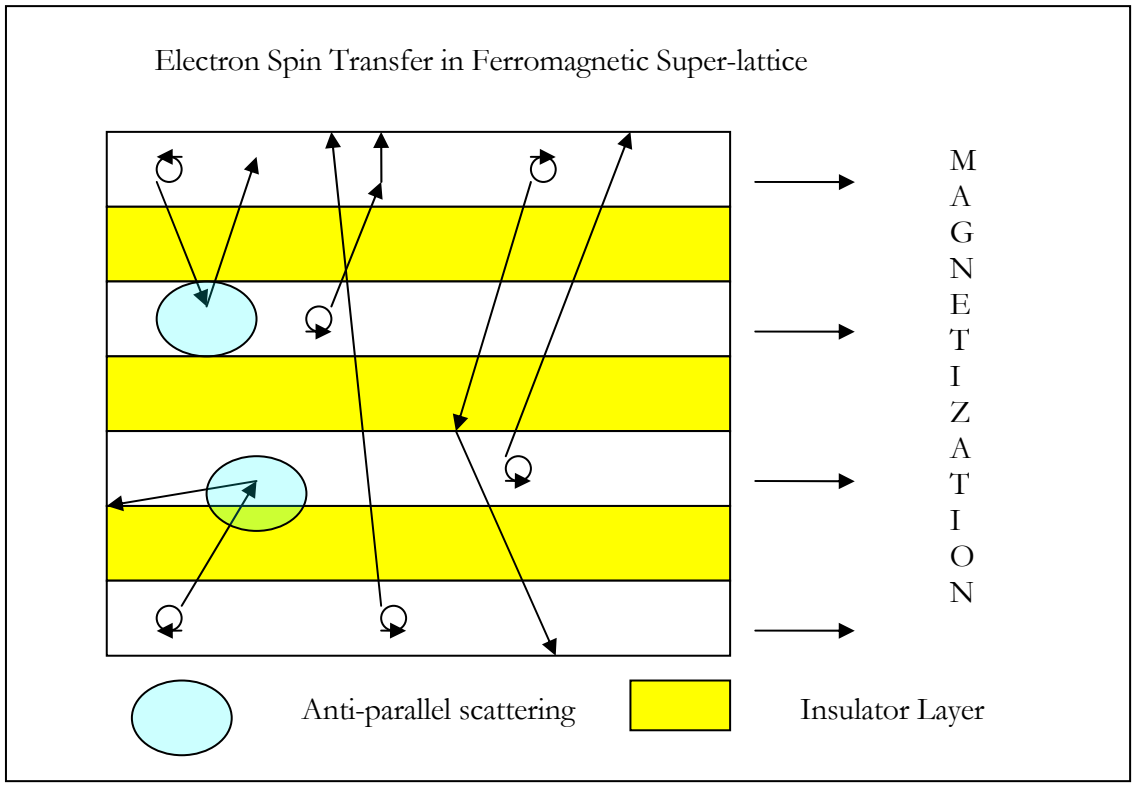

Figure 1.7 Ferromagnetic Super-Lattice GMR Scattering

From figures 1.6 and 1.7, we can see, physically, the primary cause of the giant magneto-resistance effect that is present in these ferromagnetic super-lattice configurations.

1.4 Current Research and Results

Since the advancements documented by Moodera et al. in 1995, the research world has greatly enhanced the science of spintronics. Granted, the first actual spintronics breakthrough came with the extensive Giant Magneto-resistance (GMR) work done by Baibich et al. in 1988. However, the work done by Moodera et al. showed that useful results could be achieved using a process that was not nearly as overwhelming as it was in Jullière's 1975 lab. These advancements have led the technology industry into a new era of electrical engineering and materials science.

Almost immediately following the work of the Moodera group, the magnetic tunneling junction (MTJ) was recognized as a good candidate for use in the technology world. MTJs of this type were designed and implemented to serve as magnetic sensors. The ability of these devices to change their conductance properties in such a drastic way, has led to their implementation into more than a few technology areas. Tunneling magneto-resistance (TMR) values through MTJs are now reported in the 120-160% range, using MgO barriers [5] at room temperature. When calculating these devices' effectiveness for use in technological applications, the resistance-area product becomes a key factor. In the earlier MTJ work that has been cited here, most resistance-area values were in the range of $G\Omega\text{-}\mu m^2$, but most of the recent work has come down significantly. The newer junctions that are being developed to server in Magnetic Random Access Memory (MRAM) show good magneto-resistance in the 10 $\Omega\text{-}\mu m^2$ range.

Random Access Memory (RAM) is the technology used in computers which temporarily stores instructions and data while they are being ported into and out of the

computer's processor. Generally, a piece of data to be processed will progress from the hard drive, to the RAM, to the processor, and back. In the RAM, the data has traditionally been stored in bits that are either one, or zero, depending on the electrical properties of that particular bit. As MTJ advancements were achieved. And it was recognized that a tunneling junction could easily respond to a simple shift in magnetization, a new form of RAM was born. MRAM can perform the same task as traditional RAM, but better. MRAM uses the magnetic moment direction as the means of information storage. Magnetic bits are assigned as parallel and anti-parallel magnetic orientations. These bits are then "sensed" by the change in magneto-resistance due to the presence of the magnetic orientations in the storage band. A representative diagram of an MRAM device is shown below in figure 1.8.

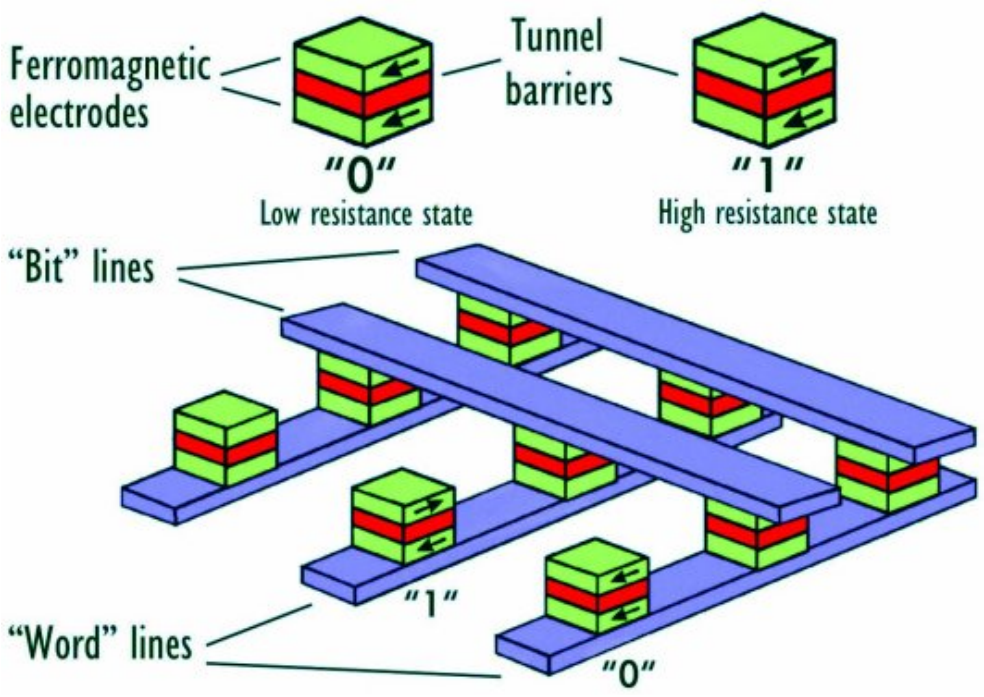

Figure 1.8 Magnetic Random Access Memory (MRAM)

These new MRAM chips have many advantages over the existing Static Random Access Memory (SRAM) and Dynamic Random Access Memory (DRAM). The first advantage of MRAM is the storage density. New MRAM designs that are currently being tested boast of memory ranges that are 500 times the current storage limitations in SRAM and DRAM. The access times for MRAM reads are also significantly smaller than those of traditional memory technologies. MRAM also provides a write time speed increase of 1000 times' current limitations. Lastly, and maybe most importantly in the computer world, MRAM technology can be transferred with the information intact, without power. Since traditional memory technology relies on electricity to set and read the bits, once power is removed from the memory stick, the information contained on the stick is lost. With MRAM, the information is stored in the magnetic orientation on the chip. If that chip is removed from one computer and added to another, the new computer has the exact same information as the old one. If this MRAM storage could serve as a complete storage solution (Hard drive and temporary memory), then you could move MRAM from one computer to another, and the new one would be in same state as the old one, without having to boot up. This is the direction that the computer industry is trying to take MRAM, and the Megneto-Tunneling Junctions are providing the technology.

Though commercial products using MTJs are currently in use, the physics of spin dependent tunneling is still far from being clearly understood. In the early research on the MTJs, it was thought that the spin polarization of the tunneling electrons and the TMR were simply reflecting the spin polarization of the electronic density of states at the Fermi level in the ferromagnetic electrodes. It now turns out that the TMR also

depends on the insulating material of the tunnel barrier and, more specifically, on the details of the electronic structure at the electrode/barrier interface. The present theories are not really quantitative yet and further theoretical developments are still needed for more reliable predictions. Another important challenge is the research of ferromagnetic materials providing higher spin polarizations than conventional metals like cobalt or iron. A few ferromagnets have been predicted to be half-metallic, that is, they present a spin polarization of 100% at their Fermi level. High TMR ratios might also be obtained with ferromagnetic insulating materials presenting a spin dependent gap and acting as spin filter for the tunneling electrons.

In a GMR or TMR device, switching the magnetic configuration changes the electrical current passing through the device. Magnetization reversal by spin transfer is an opposite effect: a spin polarized current is let into a device and the transfer of spin from the current switches the magnetic configuration of the device. This concept of magnetization reversal by spin transfer from a spin-polarized current has been introduced by Slonczewski [6] in 1995 and has been now confirmed by series of experiments (mainly on pillar-shaped multilayers). From the application point of view, reversing a magnetic moment by spin transfer without applying an external applied field can be of great interest to switch spintronic devices, MRAM for example. However the current density needed in the existing experiments is still relatively high, of the order of $10^7 A/cm^2$, and a better understanding of the spin transfer mechanisms seems necessary to obtain a significant reduction of the current density. Another effect of the same type but probably requiring a smaller current density is the displacement of a domain wall by spin transfer from a spin-polarized current.

Whereas the metallic spin devices just described provide new ways to store and read information in hard discs, tapes or MRAM, semiconductor-based spintronics may offer a greater wealth of possibilities. Why is spintronics with semiconductors interesting? First, semiconductor-based spintronics could combine storage, detection, logic and communication capabilities on a single chip to produce a multifunctional device that could replace several components. For example, it could permit a better integration between MTJ and silicon-based electronics than in the present prototypes of MRAM. The optical properties of the semiconductors are also of particular interest to transform magnetic information into an optical signal. Finally, because the manipulation of spins presents some advantages in term of speed and required power over the manipulation of charge in conventional electronics, more devices that exploit these advantages have been already proposed.

PHYSICS OF NANOJUNCTIONS

2.1 Theory of Nano-sized Tunneling Junctions

The basic defect in the classical theory of spin tunneling is that it treats the two ferromagnet (FM) electrodes as independent systems. In Jullière's model, the electron wave functions within the barrier are treated as evanescent and are assumed not to perturb the electron wave function in the other electrode. It also considers only the simple case of a square barrier, i.e. one which is unbiased, or at least where the effect of the bias voltage on the barrier shape may be ignored. As a result, this early model does not predict any barrier width or height dependence of the TMR, in clear contradiction to the measured results. The necessity of modifying Julliere's model was first realized by Slonczewski [6], who argued that because most practical barriers are relatively permeable, the wave function overlap within the barrier means that wave function matching must be considered across the entire device. Using two parabolic bands (spin up and down) shifted relative to one another by the exchange splitting, Slonczewski solved the Schrödinger equation for the wave functions of the polarized electrons tunneling across a rectangular barrier and determined the resulting conductance from the current operator. In his calculation, the polarization of the tunneling electron now depends on the height of the barrier $\mathbf{V}_b$ through an imaginary wavevector $\boldsymbol{\kappa}$ in the barrier defined by

$$\hbar\kappa = [2m(V_b - E_F)]^{1/2} \quad \text{(eq. 2.1)}$$

Using his Schrödinger solution, Slonczewski generated an equation for the polarization that involves the imaginary wavevector in the barrier.

$$P = [(k_\uparrow - k_\downarrow / k_\uparrow + k_\downarrow)] \times [(\kappa_2 - k_\uparrow k_\downarrow)/(\kappa_2 + k_\uparrow k_\downarrow)] \quad \text{(eq. 2.2)}$$

If we take Slonczewski's equation for polarization and substitute it into Jullière's equation for magneto-conductance ratio, we can obtain a more accurate solution for the tunneling magneto-resistance in the junction. This equation has a simple physical interpretation. Since the magnitude of the Fermi wavevector for a particular spin channel is proportional to the density of states at the Fermi energy, we can see that the first factor

$$(k_\uparrow - k_\downarrow)/(k_\uparrow + k_\downarrow)$$

is identical to the polarization obtained in Julliere's classical theory of tunneling, but is now multiplied by a new factor

$$(\kappa_2 - k_\uparrow k_\downarrow)/(\kappa_2 + k_\uparrow k_\downarrow).$$

Since κ ranges from 0 (low barrier) to infinity (high barrier), we can see that in the limit of high barrier height the effective polarization reduces to Julliere's result; however, for low barrier height it departs significantly and can even change sign. Hence, the matching of the wave functions across the tunnel barrier offers a plausible explanation for the observed dependence of TMR on the thickness and height of the tunneling barrier. This also shows a tunneling dependency on the choice of insulator itself.

Although Slonczewski's model provides a much more realistic treatment of the F-I-F interface than the classical theory of tunneling, its drawback is that it cannot be readily extended to more complex systems with more than one electron band. Any

rigorous model of TMR, however, has to include, or at least justify the exclusion of, the multi-orbital structure of FM electrodes. It is for this reason that a great majority of the work done to explain TMR over the last decade was based on the linear-response theory of electron tunneling. The main assumption of this theory (often referred to as the Kubo/Landauer formalism) is that the overall conductance in either spin channel for any (insulating or conducting) sample sandwiched between two electrodes can be written in terms of its total transmission coefficient [7]. The basis of the linear response theory states that the expression for the conductance in either spin channel can be written in terms of the one-electron Green's functions in the left and right planes of the tunneling junction, in a direction parallel to the current flow [8]

$$\mathbf{G^{\sigma} = 4e^2/h\ \Sigma_{k\parallel}\ [Tr(T_{\sigma}\ Im\ g^{\sigma}_{R}(E_F, k_{\parallel}) \times T^{+}_{\sigma}\ Im\ g^{\sigma}_{L}(E_F, k_{\parallel}))]} \quad \text{(eq. 2.3)}$$

The theory includes more essential components necessary to explain the observed effects than any earlier model. The Green functions for each of the k-states $\mathbf{Im\ g^{\sigma}_{R,L}(E_F, k_{\parallel})}$, (which are closely related to the densities of states) are multiplied by a matrix $\mathbf{T_{\sigma}}$ whose elements indicate the strength of the tight binding hopping between atomic orbitals in the left and right planes. Furthermore, the matrix contains an element which is responsible for the evaluation of the dependence of TMR on the height and width of the tunneling barrier, as will be shown below. Summation over the two-dimensional Brillouin zone and taking into account the different characteristics of the s-, p- and d-orbitals yields an overall conductance.

As an illustration, we can simplify the formalism and evaluate the above equation for the simple case of coherent ($k_{\parallel}$ and spin conserved) tunneling through a high barrier, assuming that the electrons originate from only one band. In this case it is found that the current in each channel is then proportional to the product of the surface densities of states of the two electrodes (as in the classical theory of tunneling), but the product is scaled by the denominator which describes the mutual interaction of the two electrodes due to overlap of the wave functions. Such a model has been used to perform numerical calculations [8] on a structure chosen to resemble a junction with Co electrodes and the result (increasing TMR with increasing barrier height $\mathbf{V_b}$, saturating when $\mathbf{V_b}$ is of the order of the bandwidth of the electrodes) is in excellent agreement with recent experimental results of Sousa *et al* [10, 11].

The observed weak variation of TMR with the barrier thickness [12] can be explained by the model if we assume that most TMR experiments are performed in the high-barrier regime. By adding a fully realistic band structure for the FM electrodes to the above model (i.e. by distinguishing between s-, p- and d-orbitals), it is possible to test whether the Kubo/Landauer formula predicts the correct sign for the polarization of the tunneling electrons. Two such calculations have been performed—one dealing with tunneling between Co electrodes through a vacuum gap [8] one through a simple step barrier [13]. The results from the first study are particularly encouraging—the calculated polarization of the tunneling electrons as the function of the tunneling vacuum gap show that, when the tunneling gap is small, (on the order of the lattice constant) the conductance is dominated by d-electrons,

and the polarization has the "wrong" sign, $\mathbf{P} < 0$ as in the classical Jullière theory of tunneling. There is a rapid crossover, however, as the width of the gap increases, and the polarization changes to positive values. Moreover, the calculated saturation value of 35–40% is in excellent agreement with the observed values [14]. The crossover occurs due to the fact that the overlap of the d-orbitals decreases with the increasing gap much faster than that of s-orbitals, and it is, therefore, s-electrons which determine the conductance in most tunneling experiments. One may, therefore, deduce that the observed sign of the polarization in junctions between ferromagnets and Al_2O_3 suggests that the sd-hybridization between the two must be weak. Going a step further in the Kubo/Landauer formalism, it is possible to consider the effect on the observed TMR of disorder in the barrier. In most tunneling experiments, the fabricated barriers are amorphous and therefore the assumption of conservation of momentum parallel to the tunneling junction ($\mathbf{k}_\parallel$) is not satisfied. Advanced studies of the effect of disorder on spin tunneling using a single orbital tight binding model and the Kubo formalism show that, in addition to the mixing of the $\mathbf{k}_\parallel$ channels, disorder also induces resonant tunneling via localized electronic states [15]. These states are formed in the barrier in the presence of impurities or defects. Resonant tunneling results in quasi-one-dimensional high-conductance channels which dominate the overall conductance if the degree of disorder is high and the barrier is thick. It then follows that the overall tunneling current, and hence the TMR, is not only determined by the intrinsic properties of the densities of states of the ferromagnet, but also, to a large extent, by the properties of the insulator. As a further test of this theory, it is useful to compare its predictions

with the experiments performed by the Moodera group [16] in which a thin layer of non-magnetic metal is inserted between one of the FM electrodes and the insulating barrier. According to the classical theory, as there is no spin asymmetry in one of the metal insulator interfaces, no TMR should be observed, which contradicts the experimental findings. In fact, calculations using the Kubo formalism by Mathon and Umerski [17], predict that the TMR should oscillate with increasing thickness of the Cu interlayer in a Co junction with a vacuum gap. For a very thin interlayer this leads to a negative TMR. This effect can be explained by considering the Fermi surfaces of Cu and Co. For the majority spin electrons in Co, the matching of the surfaces with Cu is good, whereas for the minority spins they are not. It follows that the majority spin electrons can easily cross the Co/Cu interface while the poor match for the minority spin electrons results in the formation of down-spin quantum well states in the Cu overlayer, whose loss of transport gives rise to a spin asymmetry of the tunneling current, and hence to a non-zero TMR. We can see, therefore, that the linear response theory is relatively successful in offering explanations for the many subtleties in the observed TMR effects. Many questions, however, still remain unanswered.

One of the more challenging problems when modeling TMR is the true origin of the fall in TMR with the increase in temperature. There are currently two possible explanations. The first possibility involves the mechanism of spin-flip scattering arising from magnetic impurities in the barrier, which, being an inelastic process increases with temperature. The other possible explanation suggests that the increase in temperature leads to a reduction of the overall magnetization in the ferromagnet

due to excitations of magnons. At this stage it is not clear to what extent each of these holds true. Recent work by Parkin [5] points to the former explanation. By building a single crystalline MgO barrier, Parkin drastically decreased the TMR drop off with increasing temperature. This firmly establishes that impurities in the amorphous structure of Al_2O_3 probably led to the TMR loss with rising temperature.

Another problem facing the calculations of TMR, pertains to the drop in TMR measurement with an increase in applied DC bias. The bias dependence can be accounted for by Slonczewski's model, although the initial decrease of TMR is much slower than observed [18]. An alternative explanation invokes electron–magnon scattering which flips the electron spin in the process. Since the phase space for electron–magnon scattering increases with increasing bias, the total TMR decreases. Again, at present it is unclear to what extent these mechanisms are responsible for the observed behavior.

2.2 Calculations of Nano-sized Tunneling Junctions

In 1985 Slonczewski [8] proposed a new model where the barrier height and thickness were taken into account. His model was based on the one-electron Hamiltonian within the free electron approximation. His treatment was based on Stearns [19] theory about s-d hybridized bands. The Schrödinger equation for the system is

$$[-(\hbar^2/2m_e)(\partial^2/\partial x^2)+V(x)-h(x)\sigma_z]\quad \psi(x) \quad = \quad E \qquad \text{(eq. 2.4)}$$

where **V(x)** is the potential, **h(x)σ** is the internal exchange energy, where **h(x)** is the molecular field and **σ** is the conventional Pauli operator. Slonczewski assumed that the external voltage is vanishing and the potential is zero in the electrodes and $\mathbf{V}_0$ in the barrier,

$$V(x) = \begin{cases} 0 & x < 0 \\ V_0 & 0 < x < d \\ 0 & x > d \end{cases} \qquad \text{(eq. 2.5)}$$

The molecular field is assumed to have the same magnitude in both electrode, 1 and 3, $|\mathbf{h}_1| = |\mathbf{h}_3| = h_0$, and $\mathbf{h} = 0$ inside the barrier. Slonczewski derived the conductance from this, where the molecular field between the two ferromagnets, 1 and 3, differed with an angle **μ**. The Eigen energy inside the two ferromagnets is

$$E = \tfrac{1}{2}k_\sigma^2 - \sigma h_0, \quad \sigma = \pm 1 \qquad \text{(eq. 2.6)}$$

and inside the barrier,

$$E = -\tfrac{1}{2}\kappa^2 + V_0 \qquad \text{(eq. 2.7)}$$

where $\mathbf{k}_\sigma$ is the momentum the electron, and $\mathbf{i\kappa}$ is its imaginary momentum in the barrier. From eq. 2.4 the Eigen functions $\boldsymbol{\psi}_{\sigma,r}$ are derived, one for each spin $\boldsymbol{\sigma} = \uparrow,\downarrow$ and for all the three regions *r* (1, ferromagnet; 2, barrier; 3, ferromagnet). Due to the angle shift $\boldsymbol{\theta}$ in **h**, a transformation of the wave function $\boldsymbol{\psi}$ is required at the boundary $\mathbf{x} = \mathbf{d}$,

$$\begin{pmatrix} \psi_{\uparrow,2} \\ \psi_{\downarrow,2} \end{pmatrix} = \begin{pmatrix} \cos(\theta/2) & \sin(\theta/2) \\ -\sin(\theta/2) & \cos(\theta/2) \end{pmatrix} \begin{pmatrix} \psi_{\uparrow,3} \\ \psi_{\downarrow,3} \end{pmatrix}.$$

(eq. 2.8)

The boundary conditions that the $\boldsymbol{\psi}_\sigma$ and $\boldsymbol{\partial\psi/\partial x}$ have to be continuous gives the solutions for the coefficients in $\boldsymbol{\psi}$. Then the expression for the transmissivity **T** is given by

$$T = \Im \sum_\sigma \psi_\sigma^* \frac{d\psi_\sigma}{dx},$$

(eq. 2.9)

from which the currents $\mathbf{I}_\sigma$, $\boldsymbol{\sigma} = \uparrow,\downarrow$ at zero temperature is derived,

$$\mathbf{I}_\sigma \bullet \mathbf{T}_\sigma \mathbf{V}$$

(eq. 2.10)

In the parallel orientation of the magnetization the transmissivity for an spin-up (spin-down)

electron is $\mathbf{T}_\uparrow^{\mathbf{P}}$ **(**$\mathbf{T}_\downarrow^{\mathbf{P}}$**).** Theses transmissivities have to be added to get the total transmissivity for the current.

$$\mathbf{T}^{\mathbf{P}} = \mathbf{T}_\uparrow^{\mathbf{P}} + \mathbf{T}_\downarrow^{\mathbf{P}}$$

(eq. 2.11)

The same argument holds for the antiparallel orientation of the magnetization.

$$T^{AP} = T_{\uparrow}^{AP} + T_{\downarrow}^{AP} \quad \text{(eq. 2.12)}$$

This can now be used to define the tunneling magneto-resistance (TMR).

$$TMR \equiv (R_{AP} - R_P)/R_P = (T^P - T^{AP})/T^{AP} = 2P_b^2/(1 - P_b^2) \quad \text{(eq. 2.13)}$$

The TMR diverges to infinity when the polarization goes to 1. This is sometimes called the optimal magneto-resistance. Slonczewski avoided this by instead discussing the conduction.

$$G(\theta) = G_{const}\,[1 + P^2_b \cos(\theta)] \quad \text{(eq. 2.14)}$$

where G_{const} is the mean surface conductance, and the P_b is the spin polarization defined by equation 2.2

$$P_b = [(k_{\uparrow} - k_{\downarrow}/k_{\uparrow} + k_{\downarrow})] \times [(\kappa - k_{\uparrow}k_{\downarrow})/(\kappa + k_{\uparrow}k_{\downarrow})] \quad \text{(eq. 2.2)}$$

where $k_{\uparrow}$, $k_{\downarrow}$ and κ are the electron momentum at the Fermi level in the ferromagnets

and in the barrier. The first factor in P_b is equal to the polarization defined by Jullière (equation 1.3), while the next factor

$$[(\kappa - k_{\uparrow}k_{\downarrow})/(\kappa + k_{\uparrow}k_{\downarrow})]$$

is called the interfacial factor and cannot be larger than one, or smaller than -1. This factor depends upon the barrier height (κ) and decreases the polarization when the barrier height is small. For a very small barrier, a negative polarization is obtained $(\kappa < k_{\uparrow}k_{\downarrow})$.

Equation 2.2 shows a barrier height dependence of the polarization. However, the model does not include a voltage, a temperature or thickness dependence. MacLaren et al. [20] compared the Julliere model and Slonczewski's model with the exact expression for the magneto-conductance for free electrons and a numerical calculation of band electrons in Fe tunneling through a barrier. They pointed out that the Julliere model and Slonczewski's model do not accurately represent the magneto-resistance.

However, Slonczewski's model does provide a good approximation in the thick barrier limit and for small barrier heights. Tsymbal and Pettifor [21] pointed out that the Jullieres formula (equation 1.1) agrees with the magneto-resistance for high disorder in the barrier.

2.4 Complications of Measurement

Despite the hard work of many researchers, the model for tunneling magneto-resistance is far from perfect. Many different variables are still not accounted for in a satisfactory way to properly predict the outcome of design and measurement. Thus, any future production and testing of magnetic tunneling junctions must take into account the existing models' inability to account for certain effects.

All researchers in the field of nano-sized tunneling junctions add more information to the process of developing a good model for TMR. This is what is needed at this juncture: more information. The process for designing and developing these junctions is in full swing. At this point, the most valuable contribution a researcher can make to this science is variance. In order to better understand the technology, testing methods need to be altered.

Some changes to the testing process will be presented in this thesis. These changes are meant to help overcome the deficiencies in past modeling, and to help produce new results to be added to new modeling theories.

The testing of junctions that is proposed will involve using an Atomic Force Microscope (AFM). The reasoning for this is two-fold.

Firstly, using an AFM, allows for the junctions to be accurately imaged prior to their conductance testing. This image can be used to test for pinholes in the junction, structural inconsistencies in the barrier or material, and it will give a better surface map to use for measuring the overall size of the junction. Knowing the sizes involved can greatly increase the ability to turn guess work into accuracy.

Another reason for using the AFM for these tests is the fact that the AFM is pre-designed for this sort of use. Although intended only for surface mapping and testing, the AFM has evolved over time to allow for testing of many different natures. For the purposes stated here, the design of the AFM provides one less complicated step in the measurement of tunneling junctions. In the early days of tunneling junctions, it was necessary to produce micro-sized electrodes for testing. These electrodes were difficult to produce, and may have inadvertently interfered with the tunneling process itself. With the AFM, a micro-sized tip is already in place. This tip can be used to deliver the current through the junction, eliminating the need to design and add more devices to the junctions. This allows the AFM to serve as the measurement platform for many junctions, without need for changes from junction to junction. Thus, the AFM is an important part of future research into tunneling junctions.

In the last section, it was pointed out that none of the modeling theories correctly predicts the behavior of TMR as the bias voltage is altered. The AFM helps with this as well. Since the AFM can work with external voltage and current sources inherently, it can be used to apply differing values of current and potential, to help with future modeling. In this case, a new design of the AFM allows for the introduction of AC voltage sources and AC current sources. These sources will be used to test TMR with many different settings, in the hopes of developing a better understanding of the physical phenomenon and its restrictions.

3ATOMIC FORCE MICROSCOPY

Introduction to Atomic Force Microscopy

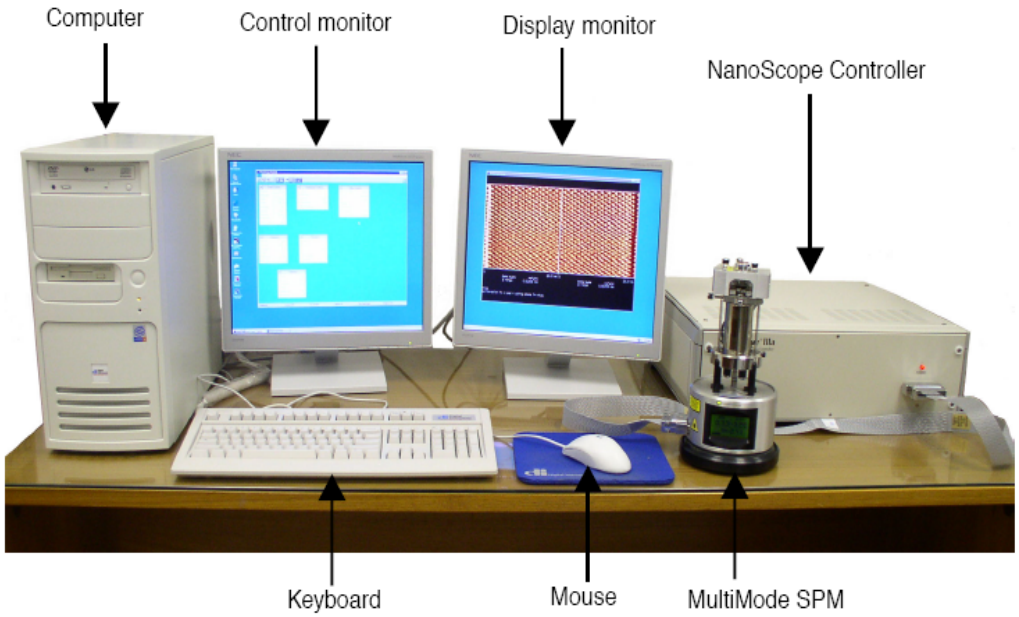

Figure 3.1 Multimode Scanning Probe Microscope (SPM) System Components

The photograph above (Figure 3.1) displays the basic hardware that comprises the Atomic Force Microscope (AFM) that is used at the University of New Orleans (UNO). Although the design and some components have been changed, this is the basic setup that was established for this device. To better understand the process of redesigning this system for the testing necessary for tunneling junctions, it is first necessary to understand the pre-existing design of the microscope system itself.

The AFM at UNO is a Veeco Digital Instruments Multimode Scanning Probe Microscope (MM-SPM). This device is designed to image small samples using

interchangeable scanners. This microscope can produce images from the atomic scale up to 175 •m in size.

The MM-SPM is designed around a stationary probe. The probe itself does not move in the process of scanning, but instead the samples are scanned back and forth beneath the probe. All samples are fixed to a 1.5 cm metal disc (called a puck) and then magnetically attached to the top of the scanner tube. As the scanner tube adjusts back and forth, the sample moves right along with it, allowing the probe to extract information from the surface of the sample, much the way a needle extracts information from a phonograph record.

All information gathered from the sample surfaces is electronically derived and rendered. This is due to the fact that many of the size features imaged with the MM-SPM are below the visible wavelength of light. For this reason, the microscope is controlled by a computer running a custom built Veeco software package. The software is responsible for the settings and functionality of the microscope, as well as for the derivations and rendering of the surface images.

The actual imaging of the samples is performed using the Atomic Force Microscope (AFM) system. This is a subsystem of the MM-SPM. The AFM system is comprised of two main components: 1) the scanner; 2) the AFM detection system. The scanner houses the piezoelectric transducer. The piezo element physically moves the sample in the X, Y and Z direction. The detection system consists of a laser which generates a spot of light that is reflected off of a micro-fabricated cantilever onto a mirror and finally into a photo detector (see Figure 3.2). The position of the spot is determined by circuitry which generates a voltage from the difference

between the photodiode segments (A - B). The circuit outputs a voltage ranging from +10V to -10V depending on the position of the spot on the two photodiodes.

The AFM system maintains the tip at the end of the cantilever in contact with the sample surface. The sample is scanned under the tip in X and Y. Features on the sample surface deflect the cantilever, which in turn change the position of the laser spot on the photodiodes. This position change is read by the feedback loop. The feedback loop moves the sample in Z to restore the spot to its original position.(see Figure 2.4a).

1. A flat portion of the sample surface is scanned beneath the tip left-to-right, maintaining the laser beam at the center of the photodiode array.
2. As the tip encounters a raised feature, the cantilever is pushed up, deflecting the laser beam upward onto the "A" portion of the array. With the "A" photodiode receiving an increased portion of the laser light, its voltage increases while portion "B" sees a light decrease.
3. The vertical deflection voltage differential is sensed by the feedback electronics, causing a dropped voltage to the Z peizo crystal, which causes the piezo to retract. As the Z piezo retracts, the cantilever re-centers the laser beam onto the photodiode array.
4. As the tip encounters a decline in the sample topology, the tip drops. This directs more of the beam onto the "B" portion of the photodiode array. With the "B" photodiode receiving an increased portion of the laser light, its voltage increases while portion "A" sees a light decrease.

5. Again, the vertical deflection voltage differential is sensed by the feedback electronics, increasing the voltage to the Z piezo crystal, causing the piezo to extend. As the piezo extends, the tip is pushed down until the laser beam re-centers on the photodiode array.

Figure 3.2 below displays this control mechanism, and the step by step adjustments performed by the piezo element and the feedback electronics.

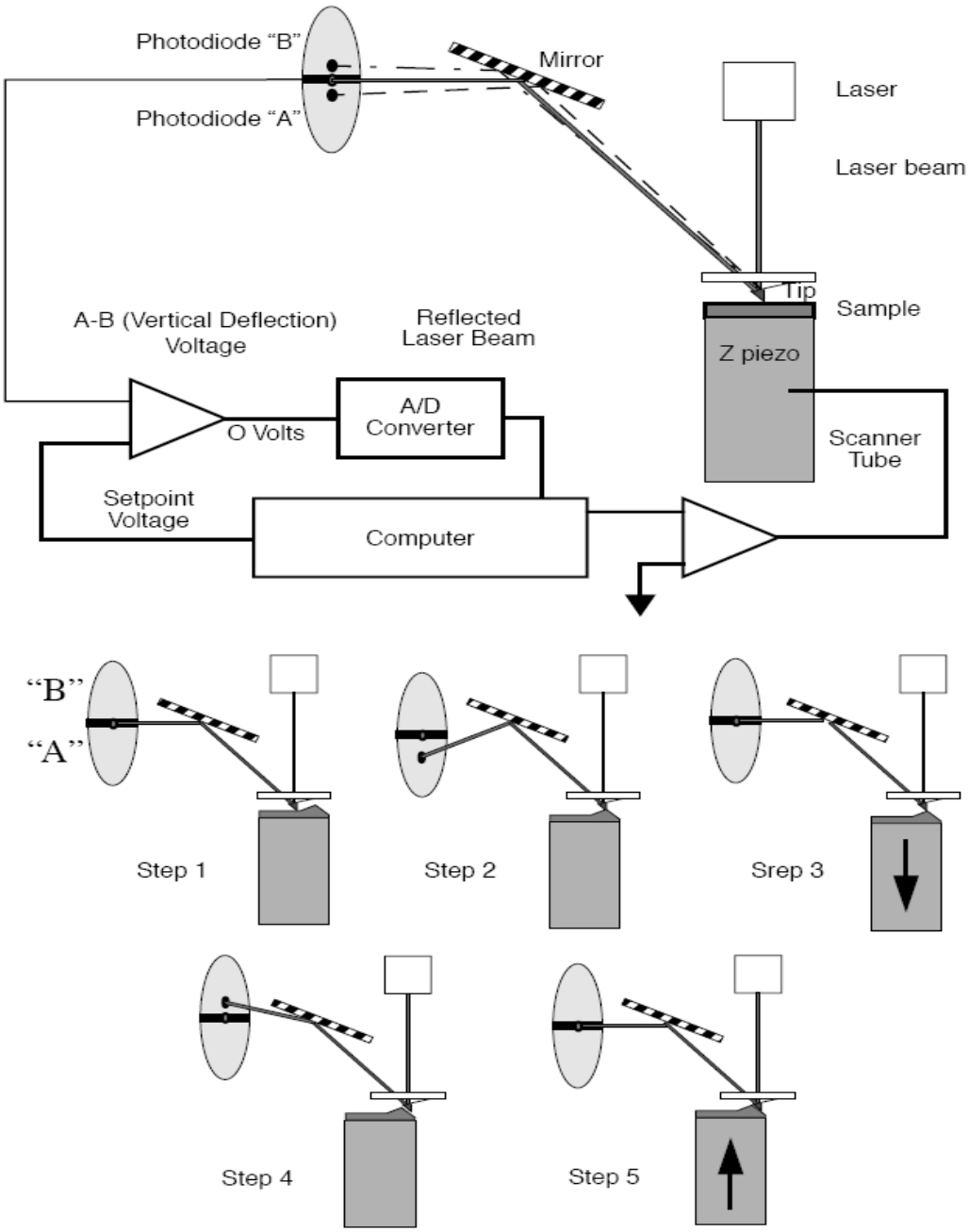

Figure 3.2 AFM Feedback Control Mechanics

3.2 Transforming AFM to C-AFM

When trying to discover the physical structure, and surface properties of a sample, the standard multimode scanning probe microscope (MM-SPM) functionality does an outstanding job. Prior to making modifications for the specific testing of magnetic tunneling junctions, the MM-SPM was used extensively to image samples that had been created for other reasons. As the intent to study MTJ became known, it became clear that more testing was going to be needed. Since the Atomic Force Microscopy (AFM) manufacturer provided an add-on kit to measure current and resistance through a sample, this seemed the way to go.

Funding became a problem at this point. The additional equipment required to transform the AFM into a Conducting Atomic Force Microscope (C-AFM) was determined to be cost prohibitive. Regardless, the ability to use one device to both image a sample, and measure that sample's I-V properties was entirely too tempting to ignore. As a consequence, a project was begun to convert the existing AFM into C-AFM.

The first big obstacle to measuring conduction with the AFM was that the AFM was designed for measurements of the magnetic or force variety. There was some budget money available to make some small equipment changes to the AFM system, and so an electronics extender module and a special electric cantilever holder were purchased. Along with this purchase, conductive cantilever tips were also obtained. These parts formed the first major change of the AFM to C-AFM capability. This gave the AFM the ability to perform what is called Electric Force Microscopy (EFM).

These changes required changes in both the hardware and the software of the MM-SPM. Figure 3.3, below shows the process of altering the internal electronics of the MM-SPM body to accommodate the addition of the extended electronics module and EFM functionality of the microscope. Figure 3.4 displays the base plate of the MM-SPM body, and the jumpers that needed configuration and rewiring. Figure 3.5 shows the diagram of the jumper settings, wiring and associated circuit diagram for these configuration changes.

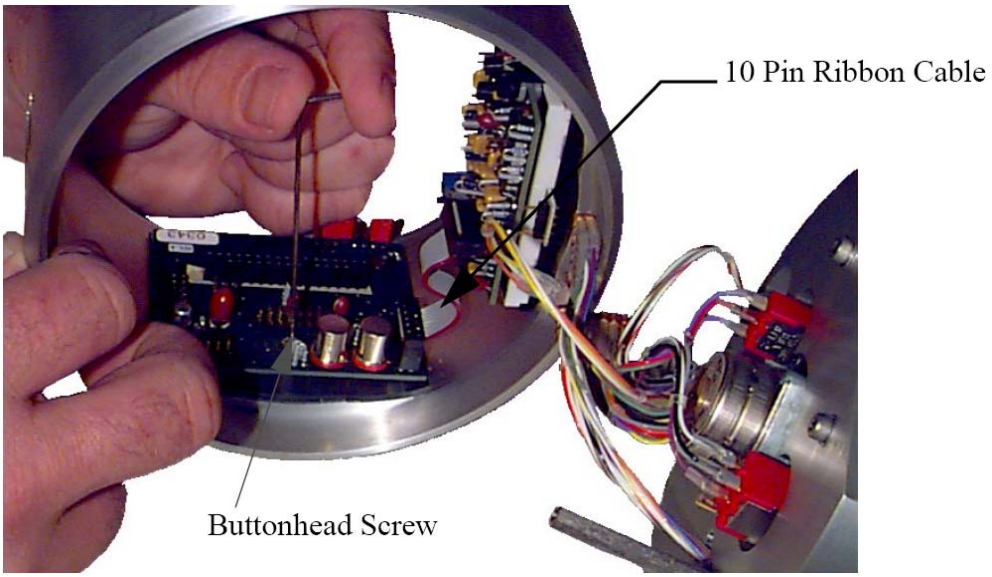

Figure 3.3 Installing Extended Electronics Module in AFM

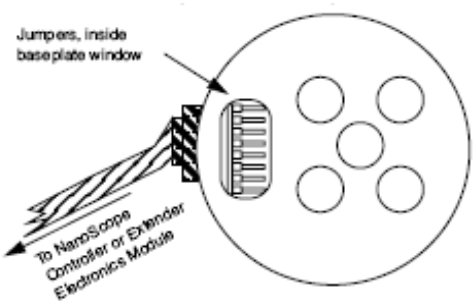

Figure 3.4 Multimode Base Plate Showing Configuration Jumpers

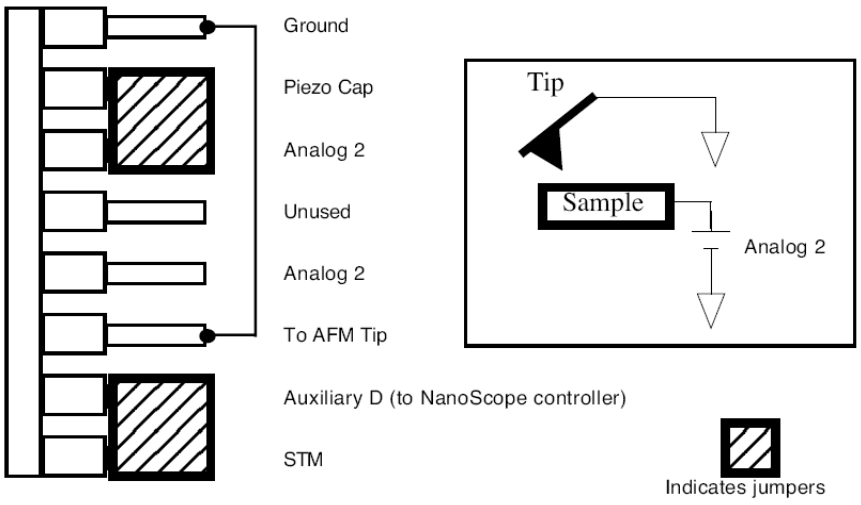

Figure 3.5 Wiring and Jumper Changes Made to Allow Voltage Through Tip

EFM is analogous to standard Magnetic Force Microscopy (MFM - one of the basic functions of the AFM), except that the gradients that are sensed are due to electrostatic forces, not magnetic forces. When EFM is employed, the cantilever is vibrated by a small piezoelectric element that is at or near its resonant frequency. Any additional force gradient changes the resonant frequency in the cantilever, triggering an adjustment in the cantilever. Attractive electric forces cause reductions in the cantilever's resonant frequency. Conversely, repulsive electric forces cause an increase in the resonant frequency of the cantilever. Figure 3.6 shows the circuit diagram for this frequency control.

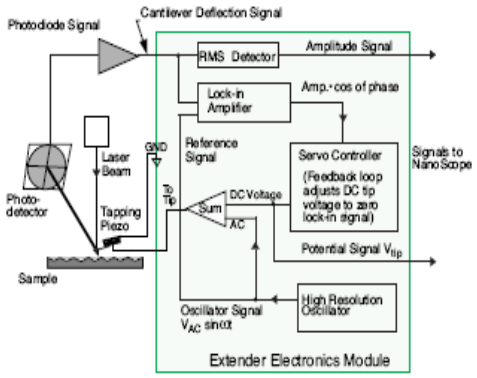

Figure 3.6 Circuit Input/Output Diagram of EFM with Extender Module

These cantilever resonant frequency changes can be detected in any of three ways: phase detection, frequency modulation, or amplitude detection. Since all of these methods rely on a change in the cantilever resonant frequency due to vertical force gradients, the electronics extender module is a necessary addition. The electronics extender module provides the feedback and signal enhancement necessary to allow this gradient detection.

Figure 3.7, below shows how the detection of vertical force gradients adjusts the resonant frequency of the cantilever. The gradients essentially act like a spring that changes the resonant frequency through tension and compression type functionality.

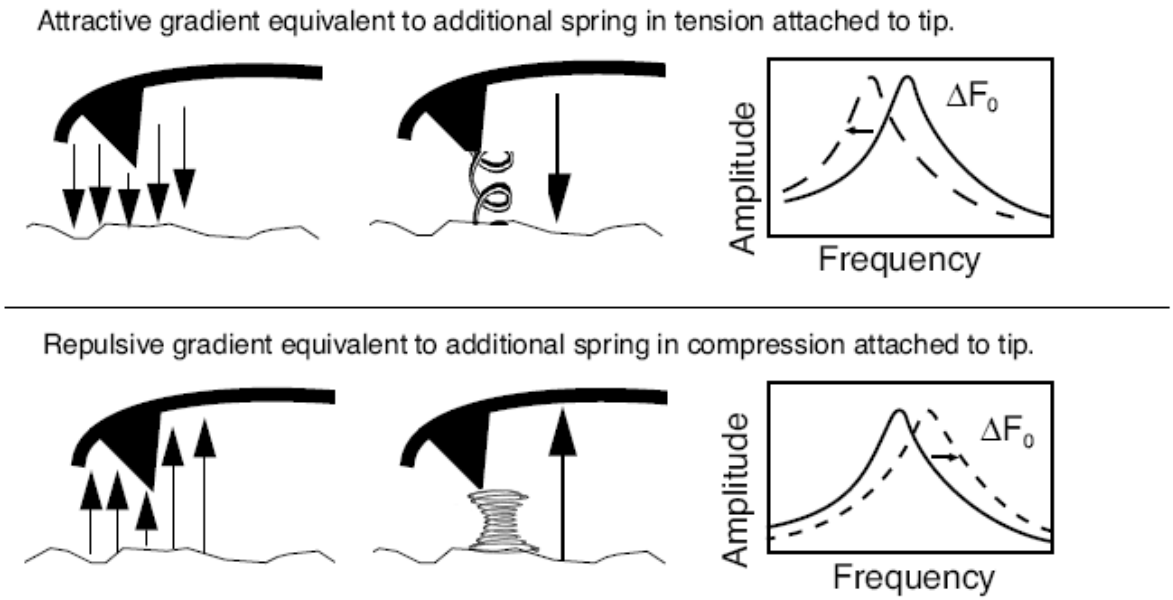

Figure 3.7 Gradients Adjust the Resonant Frequency of the Cantilever

Initially, attempts were made to use the AFM with the extended electronics module to perform some rudimentary current-voltage measurements. The software that controlled the AFM with the extended electronics module allows for the user to select an input DC voltage to be applied to the tip of the cantilever. Unfortunately, this DC input is not useful as a measurement of bias voltage. After performing several measurements with the AFM in EFM mode, it was discovered that the current passing through the sample was higher than should be expected. After much consternation, study and conferencing with the makers of the AFM, it became clear that the DC voltage signal applied to the tip mixes with the AC voltage signal that is sent to the cantilever to adjust the frequency of oscillations. As a consequence, this method could not work, as is, for our measurement needs.

Thinking in a perfect world, the best way to ensure that the voltage signal applied to the sample is not compromised, is to create that signal ourselves. In order to insert a custom signal, one last piece of equipment was installed on the MM-SPM. The Nanoscope Signal Access Module (SAM) was obtained from Veeco, the manufacturer of the MM-SPM system. Figure 3.8 shows a picture of the SAM, so that one can see all of the input and output capabilities provided by this device.

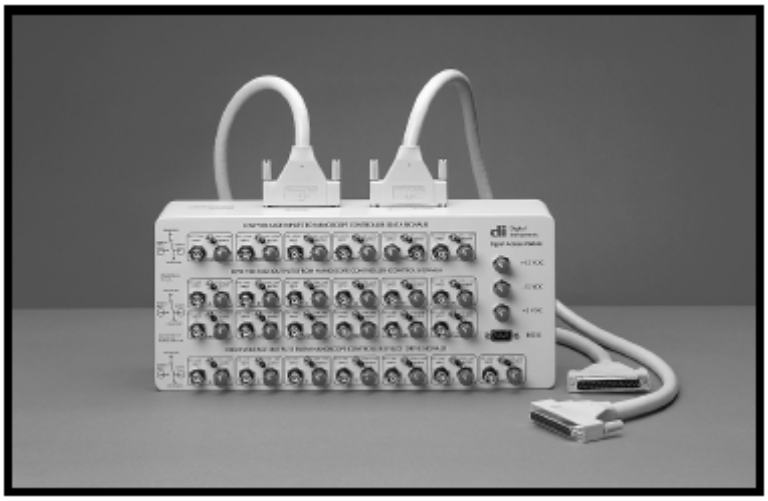

Figure 3.8 Nanoscope Signal Access Module (SAM)

The functions and abilities of the SAM are plentiful. For the purposes of working with and measuring tunneling junctions, the customized input and output terminals allow for an isolated current-voltage circuit. In addition to direct connections to allow the user to connect a voltage or current source directly to the tip of the cantilever, the SAM also allows for connecting a meter to read the signals that are generated inside the MM-SPM. This allows for direct control of the piezo drive signal, the voltage applied to the tip, and the feedback signal. Also, the piezo voltage can be read alongside the tip voltage, allowing the user to separate these two signals. The addition of the SAM required that both hardware and software changes be made to the

Nanoscope system. Figure 3.9, below highlights the changes that were made in the wiring and jumpers of the microscope to accommodate the increased functionality of the SAM. A SAM can be configured into your system in different locations, depending on the results you hope to obtain. Figure 3.10 displays where the SAM was wired into the existing equipment scheme in this particular setup.

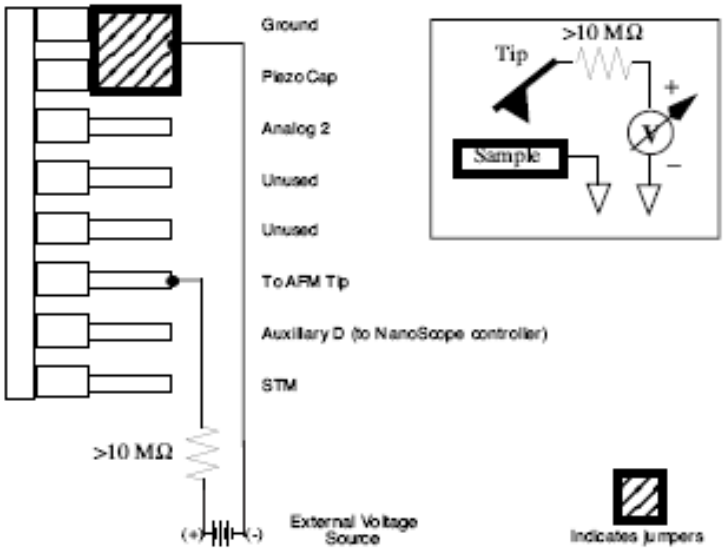

Figure 3.9 Wiring and Jumper Changes Made to Allow Signal Access Module

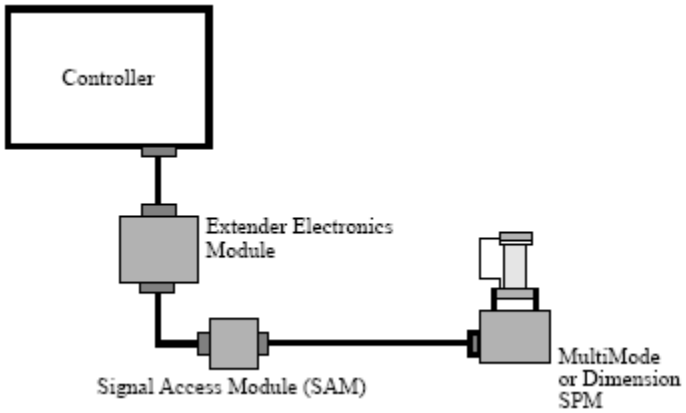

Figure 3.10 SAM Location Within New Design

With the SAM in place, testing and measurements continued. The software that controls the system has an almost cumbersome number of settings to be configured. Since each system is designed, built and configured differently, there is no standard setup for all of the settings in both the software and hardware. Thus, a significant amount of time was invested to learn the optimum settings for the software and the hardware, at each level of measurement and testing.

In the end, it was determined that the settings that allow for accurate imaging and measurement of samples in the 10 – 100 •m range are very different from the settings that work for samples below the .5 •m mark. The frequencies needed to measure the larger samples need to be significantly reduced (multiple factors) to accommodate the smaller samples. Also, the set point voltages and the scan rates needed to be adjusted accordingly. Finally, good baseline settings were achieved for the size of samples that are expected to be measured by this device in the future. Figure 3.11 shows the settings screen that maximizes the imaging and measurement of a sample in the 125 nm range.

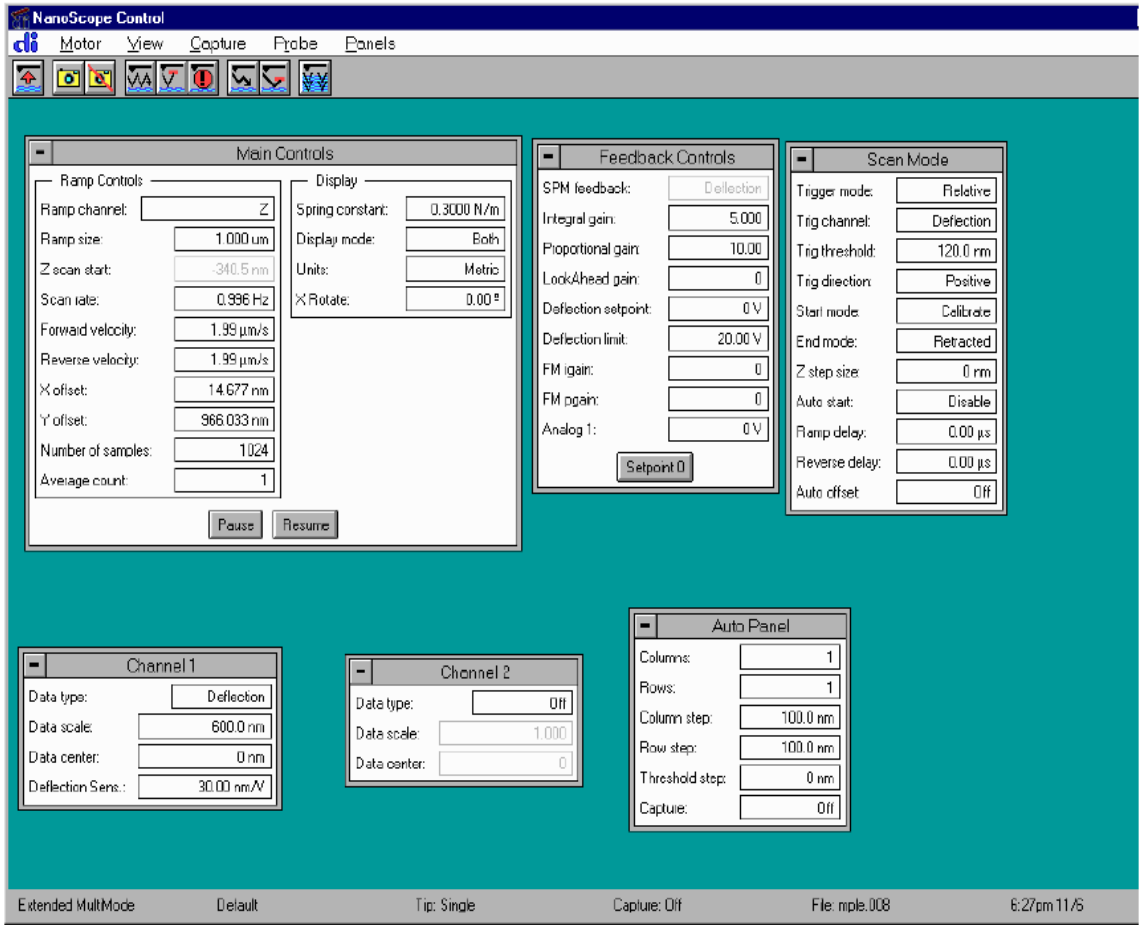

Figure 3.11 Nanoscope Software Settings for 125 nm Sample Size

3.3 Modifying C-AFM Design for Accuracy

The previous section discussed the trials and tribulations of converting an Atomic Force Microscope (AFM) into a Conductive Atomic Force Microscope (C-AFM). This system design created a device which could be used to image a given sample, and measure its I-V characteristics, without having to move the sample from one device to another. The method for measuring I-V characteristics is not built into the system inherently, though. In order to maximize the accuracy of the measurements, some design work, outside of the microscope, needs to be done.

Initially, the imaging process (based on sample size) had to be perfected using the new extender electronics module and Signal Access Module (SAM). Once this had been achieved, focus was paid to the ability to measure I-V characteristics through the samples. With much assistance from the MM-SPM manufacturer, a basic method for testing the resistance through a sample was developed. The signal that was measured was far from what was expected, but it was stable, and responded in the right way, to our input changes.

Over time, small changes were made to eliminate sources of noise in the measurement system, to produce a better method of providing a current to the sample and to better read the current actually crossing the sample. After a series of small changes, it became obvious that perhaps the design had evolved in a direction that was not going to become what it needed to be. The design, by this point, even contained wires that were directly attached to the sample surface, and wired into the ground feed for the base of the microscope. This design was unwieldy, and yielded results that were noisy.

Making a major change in the design was the only reasonable option. A new design, involving lock-in amplifiers, would allow the noise in the output signal to be filtered. Also, using an input voltage, instead of an input current, could make the measurements more stable. This stability could be achieved by using an external resistor in the circuit, prior to the introduction of the signal into the microscope. Both of the changes have been implemented in the new system design.

Firstly, the voltage that is applied to the tip for measurement of the sample needs to be distinguished from any other random voltage signals that may be introduced into the system at some point or another. Everything in the room contributes some amount of noise to the signal, so it is important to be able to verify that the output measured was generated by the input signal. To accomplish this, the new system design incorporates lock-in amplifiers. The lock-in amplifiers allow for a voltage source to be applied, at a given frequency. This frequency can then be isolated at the output of the system, and measured by itself. Through careful frequency selection, this will allow the voltage signal that is applied to the tip to be measured independently from all other signals in the system.

The second big change in the new design involves the introduction of a voltage source instead of a current source. This new voltage source also includes an external resistor, to lower the current entering the microscope. The tips used to measure the samples cannot handle a current in excess of 10 •A. This is a severe limiting factor when working with a current input device. To overcome this, the new design incorporates a 10 mV AC source that includes a frequency control selector. Thus, AC voltage can be introduced into the system, at a given frequency. The voltage source

directly feeds a resistor, which then feeds the signal to the SAM, and ultimately, the tip of the AFM. Through this method, the current is kept below the maximum allowed value and the voltage input is of a known value at a known frequency. Another positive here is that the resistance of the entire leg is already more than 100 Ω, so any small amount of resistance encountered throughout the system will be on the order of 10^{-2} in the total resistance measurement. This makes it easier to see the actual resistance due to tunneling magneto-resistance.

Figure 3.12 shows the circuit diagram of this new system design. In the figure, both lock-in amplifiers are shown, along with the locations of their reference signal lines. The reason two lock-in amplifiers are used in this design is to isolate the signal just as it goes through the Nanoscope, and separately to compare the signal that entered the entire system with its reference signal.

Testing of this new system for measurement has already begun, and this system is prepared to measure magneto-tunneling junctions as soon as they are available. The separated signals in this design provide a good test-bed for newly created junctions. The analog lock-in amplifier will serve to ferret out pinholes and impurities in the samples, and the digital lock-in amplifier will provide accurate measurements of the tunneling magneto-resistance.

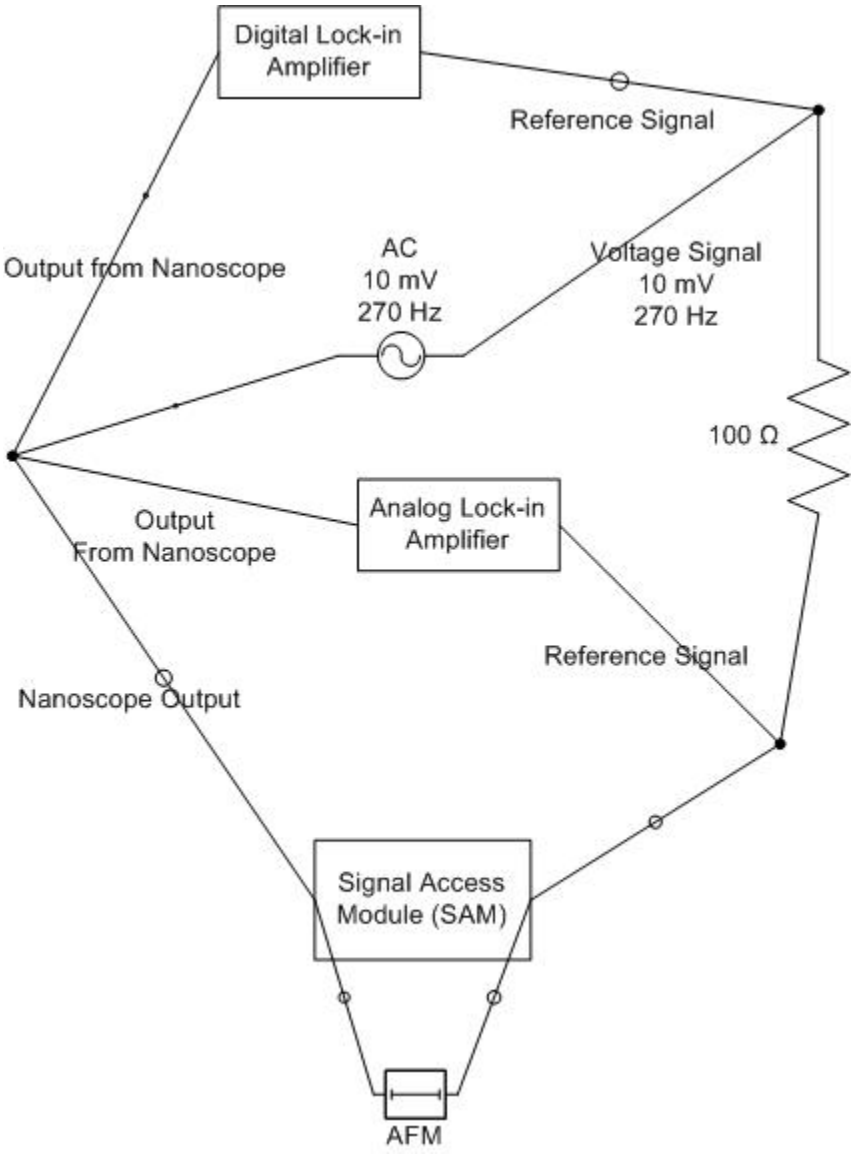

Figure 3.12 Circuit Diagram of New Measurement System

As stated before, imaging with the AFM has become more and more important to the process of measuring tunneling junctions. Figures 3.13, 3.14 and 3.15, show three different images obtained through the use of the AFM. Figures 3.13 and 3.14 display nanorods amplitude imaged with the AFM. Figure 3.15 shows the same rods, images in phase detection mode, at a much smaller scan size. With the smaller scan size, one

can see the atomic detail on the surface of the sample. This allows for the selection of specific areas for testing.

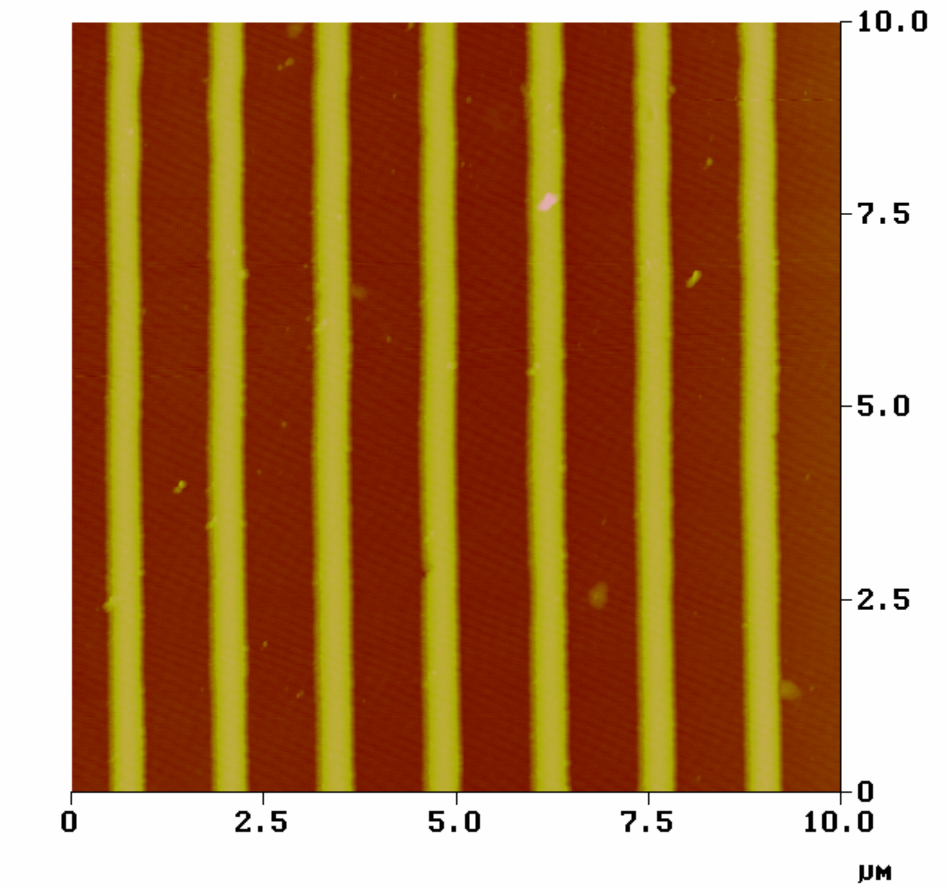

Figure 3.13 Nanorods Imaged with AFM 1

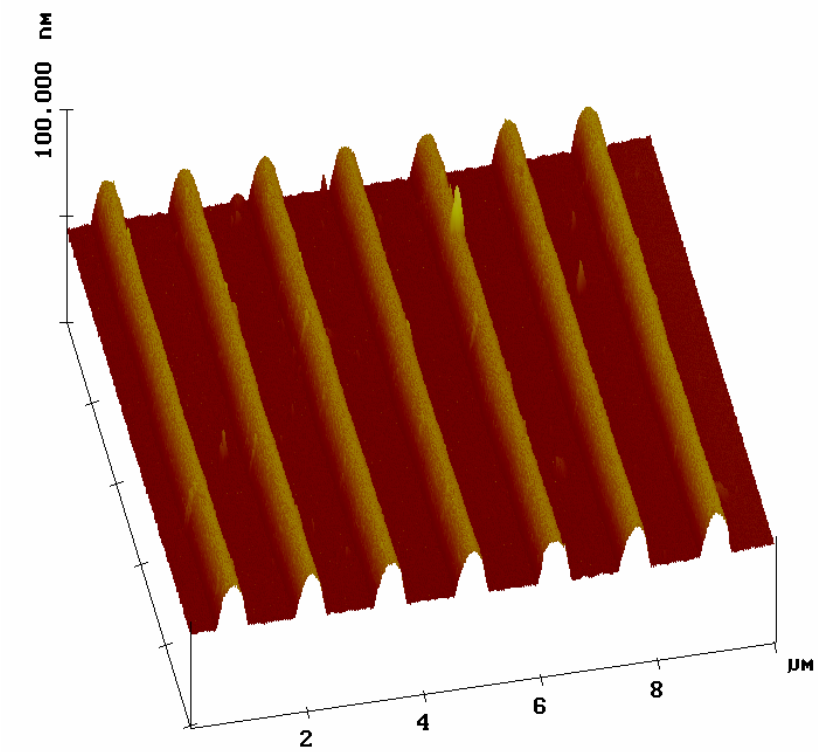

Figure 3.14 Nanorods Imaged with AFM 2

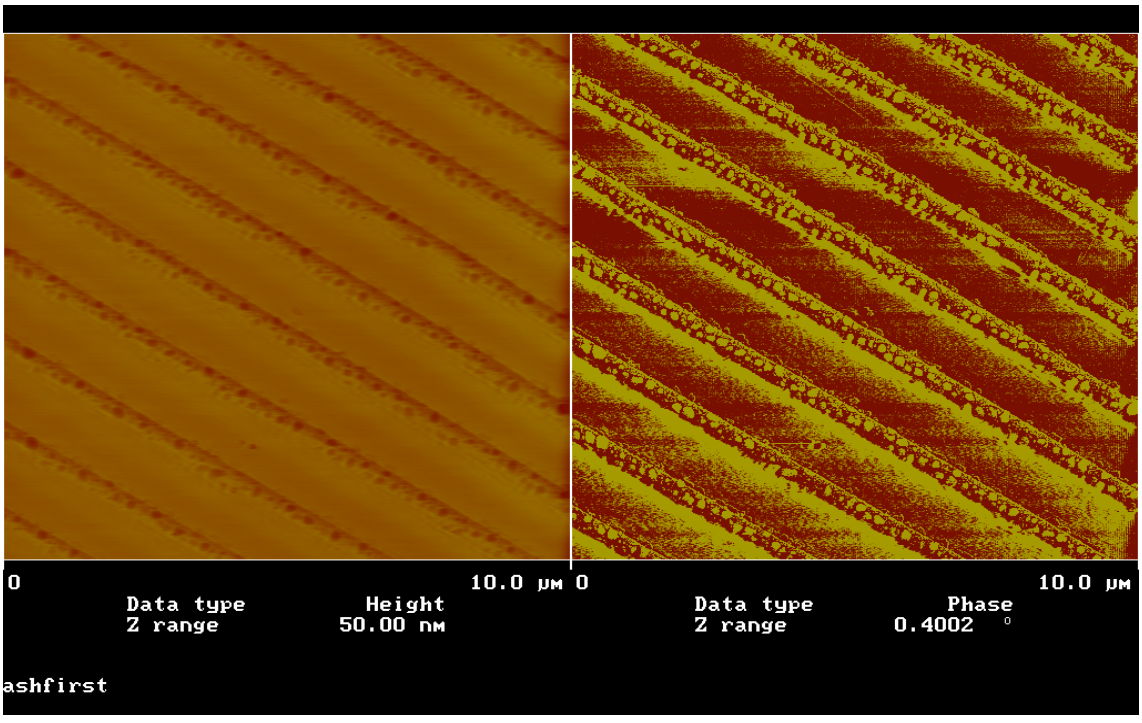

Figure 3.15 Nanorods Imaged with AFM 3

An important part of the measurement process is the ability to identify, isolate and touch individual structures in a sample. Now that the AFM can be restricted to a .5 nm square scan size, knowing the map of the surface becomes very important.

NANO-TUNNELING JUNCTION MODELING

4.1 Ferromagnet-Insulator-Ferromagnet Model

Throughout the course of this thesis, most of the focus has been on planning for the production of magneto-tunneling junctions (MTJ). Without some idea of what to expect to measure, and what results should be reasonable, the process of researching these devices may be trivial, at best. For this reason, much of the preparation time has been spent trying to model the values that would be considered consistent with the junctions that will be built. Obviously, it would be impossible to exactly predict the outcome of any experiment, but a decent attempt at modeling is a good place to start, nonetheless.

Here, some theorized junction modeling will be presented. In section 2, theories were presented that have been reasonably accepted in the research community, and have some resemblance to experimental results. The equations and calculations displayed here are meant for approximating future results in the laboratory. While these values may not be exact, the expectation is that they will provide a good basis for which to evaluate our processes for development, handling and measurement.

Recalling equation 2.4 from earlier, this single-particle Hamiltonian can be solved.

$$[-(\hbar^2/2m_e)(\partial^2/\partial x^2)+V(x)-h(x)\sigma_z] \quad \psi(x) \quad = \quad E \qquad \text{(eq. 2.4)}$$

Assuming that the exchange energy **h(x)** is zero inside of the barrier, and that the potential function disappears inside the ferromagnetic layers, we achieve equation 2.5.

$$V(x) = \begin{cases} 1 & x < 0 \\ V_0 & 0 < x < d \\ 0 & x > d \end{cases}$$ (eq. 2.5)

Instead of approaching this solution with these boundary conditions as Slonczewski did, we will take the approach of the direct tunnel current for spin. This method depends on the Fermi-Dirac distribution function and the transmission probability, as laid out by Duke [22].

$$\frac{I_\sigma}{A} = \frac{e}{h}\int_{-\infty}^{\infty} dE[f(E) - f(E+eV)]\int \frac{d^2k\|}{(2\pi)^2} T_\sigma(E,k\|)$$ (eq. 4.1)

Here, **A** is the contact area, $\mathbf{f(E_x)}$ is the Fermi-Dirac distribution function and $\mathbf{T_\sigma}$ is the transmission probability for the barrier. When the barrier takes on a square shape, the transmission probability function takes on a simple form, below.

$$T_{\sigma\sigma'} = \frac{16 m_1 m_3 m_2^2 k_{1\sigma} k_{3\sigma} k_{2\sigma}{}^2}{(m_2^2 k_{1\sigma}^2 - m_1^2 k_{2\sigma}^2)(m_2^2 k_{3\sigma}^2 - m_3^2 k_{2\sigma}^2)} e^{-2\kappa w}$$ (eq. 4.2)

Assuming that $m_1 = m_3$ and that $k_{1\sigma} = k_1$ and $k_{3\sigma} = k_3$ and $k_{2\sigma} = i\kappa$, then this equation can be changed. Here, w is the width of the tunneling barrier and the k-values are the momenta normal to the barrier.

$$T_{\sigma\sigma'} = \frac{16 m_1{}^2 m_2^2 k_1 k_3 \kappa^2}{(m_2^2 k_1^2 + m_1^2 \kappa^2)(m_2^2 k_3^2 - m_3^2 \kappa^2)} e^{-2\kappa w}$$ (eq. 4.3)

If we recall equation 2.14, the value of G_{const} is this value for $\frac{I_\sigma}{A}$ that we see in equation 4.1.

$$\mathbf{G(\theta) = G_{const}\,[1 + P^2{}_b \cos(\theta)]}$$ (eq. 2.14)

Solving the integrals in equation 4.1 for the transmission probability, the yielded value for $\frac{I_\sigma}{A}$ comes out to:

$$G_{const} = \frac{e^2\kappa}{\pi^2 hw}\left[\frac{\kappa(k_\uparrow + k_\downarrow)(\kappa^2 + m_2^2 k_\uparrow k_\downarrow)}{(\kappa^2 + m_2^2 k_\uparrow^2 k_\downarrow^2)(\kappa^2 + m_2^2 k_\uparrow^2)}\right]^2 e^{-2\kappa w} \qquad \text{(eq. 4.4)}$$

It is important to note that m_2 is the *effective* mass in the barrier. The value of **κ** can be obtained from the $\mathbf{k}_\uparrow$ and $\mathbf{k}_\downarrow$ values, as $\boldsymbol{\kappa} = \mathbf{k}_\uparrow\, \mathbf{k}_\downarrow$**.** This comes from the wide barrier model **κw>>1**

$$\mathbf{K = [2m_2(U_0 - E)/\hbar^2]^{1/2}} \qquad \text{(eq. 4.5)}$$

If we take the value of **κ** deter substitute it into equation 4.4, with some values taken from tables, and some assumed, a value for $\mathbf{m_2}$ can be approximated. This value can then be used to find the polarization value at the barrier, $\mathbf{P_b}$. The effective mass value obtained here, $\mathbf{m_2}$**,** will alter the second term in equation 2.2.

$$\mathbf{P_b = [(k_\uparrow - k_\downarrow/k_\uparrow + k_\downarrow)] \times [(\kappa_2 - m_2^2 k_\uparrow k_\downarrow)/(\kappa_2 +} \qquad \text{(eq. 4.6)}$$

From this calculation for $\mathbf{P_b}$, we can estimate the value of the tunneling magneto-resistance by using equation 2.13.

$$\mathbf{TMR \equiv (R_{AP} - R_P)/R_P = (T^P - T^{AP})/T^{AP} = 2P_b^2/(1 - P_b^2)} \qquad \text{(eq. 2.13)}$$

Again, it is important to remember that these values require approximations in the theoretical arena. Once junctions are built, some of the guesses provided in calculations can be replaced with actual observed values, and then these calculations

for TMR should provide a reasonable range of outcome values for variable width and different materials.

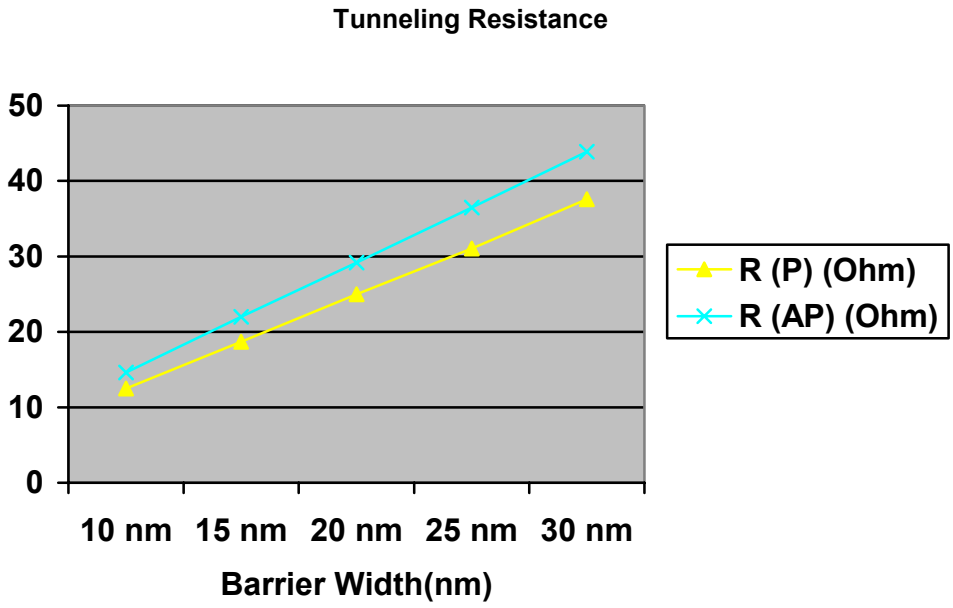

Figure 4.1 Table of Resistance Approximation Fe-Al_2O_3-Fe Junction

Figure 4.1, shown here, displays some calculated values for the conductance through a .1cm x .1cm Fe-Al_2O_3-Fe junction, using the model presented in this section. This graph clearly shows how the barrier width influences the resistance for smaller values of the barrier width. Once the barrier width exceeds the mean free path of the electron spin, this resistance falls off dramatically.

Conclusion

As the world of technology becomes more complicated, it is more and more important that science stay ahead of the technological needs. The quantum mechanical properties of the electron hold promise for new breakthroughs for years to come. Magnetic Tunneling Junctions (MTJ), which are dependent on the spin of the electron, provide new challenges for researchers, and new hope for advancements.

In order to fully understand the intricacies of tunneling junctions, it is important to be capable of correctly measuring these junctions. This thesis outlines a unique method for measuring Tunneling Magneto-Resistance (TMR) in MTJ devices. To truly claim a complete knowledge of a device, it is imperative to be completely sure of the values measured for that device.

The use of atomic force microscopy to measure the magneto-resistance in a tunneling junction is not the established best method. However, because the values of resistance and TMR in these junctions is on the order of 10-10000Ω, the C-AFM is more than capable of testing these devices. More importantly, the AFM will allow for the imaging of the devices, as well as I-V measurements. This allows for the detection of impurities, pinholes and any surface features that may interfere with the value of the measurement.

As I look forward to building tunneling junctions of my own, and discovering my own phenomena to manipulate and learn from, I feel confident that the methods I have developed for testing my junctions is consistent.

References

[1] M. Jullière, *Phys. Lett. 54A* (1975) 225.

[2] J. S. Moodera et al., *Phys. Rev. Lett. 74* (1995) 3273

[3] M. N. Baibich et al., *Phys. Rev. Lett. 61* (1988) 2472

[4] G. Binash, P. Grünberg, F. Saurenbach and W. Zinn, *Phys. Rev. B39* (1989) 4828

[5] S. S. P. Parkin et al., *N. Mat. 3* (2004), 862-867

[6] J. Slonczewski, *J. Mag. Mag. Mat. 159* (1996), 1

[7] Landauer R., *IBM J. Res. Dev. 32* **(**1988), 306

[8] Mathon, J., *Phys. Rev. B 56* (1997), 11810

[9] Parkin S. S. P., More N. and Roche K. P. *Phys. Rev. Lett. 64* (1990), 2304

[10] Sousa et al., *J. Appl. Phys. 85*, (1999), 5258

[11] Sousa et al., *Appl. Phys. Lett. 73*, (1995), 3288

[12] Moodera J. S., et al., *Appl. Phys. Lett. 70* (1997) 3050

[13] MacLaren J. M., Zhang X.G. and Butler W. H., *Phys. Rev. B 56* (1997) 11827

[14] Meservey R. and Tedrow P. M., *Phys. Rep. 238* (1994) 173

[15] Bratkovsky A. M., *Phys. Rev. B 56* (1997) 2344

[16] Jansen R. and Moodera J. S., *Appl. Phys. Lett. 75* (1999) 400

[17] Mathon J. and Umerski A., *Phys. Rev. B 60* (1999) 1117

[18] Xiangdong Zhang, et al., *Phys. Rev. B 56* (1997) 5484

[19] M. B. Stearns, *J. Magn. Magn. Mater. 5*, (1977) 167–171

[20] J. M. MacLaren, X.-G. Zhang, and W. H. Butler, *Phys. Rev. B 56* (1997) 11827–11832

[21] Tsymbal R. Y. and Pettifor D. G., *Phys. Rev. B 58* (1998) 432–437

[22] Duke C. B., *Tunneling in Solids*~Academic, New York, 1969

APPENDIX

A.1 Acronyms Used in Text

AC	**Alternating Current**
A/D	**Analog to Digital**
AFM	**Atomic Force Microscope**
C-AFM	**Conductive Atomic Force Microscope**
DC	**Direct Current**
DOS	**Density of States**
DRAM	**Dynamic Random Access Memory**
EFM	**Electric Force Microscope**
F-I-F	**Ferromagnet-Insulator-Ferromagnet**
FM	**Ferromagnet**
GMR	**Giant Magneto-Resistance**
I-V	**Current-Voltage**
MFM	**Magnetic Force Microscope**
M-I-M	**Metal-Insulator-Metal**
MM-SPM	**MultiMode Scanning Probe Microscope**
MRAM	**Magnetic Random Access Memory**
MTJ	**Magnetic Tunneling Junction**
RAM	**Random Access Memory**
RMS	**Root Mean Square**
SAM	**Signal Access Module**

SPM	**Scanning Probe Microscope**
STM	**Scanning Tunneling Microscope**
TMR	**Tunneling Magneto-Resistance**

VITA

Donald James Scherer, II was born in New Orleans, Louisiana in 1972.

He is a veteran of the United States Marine Corps.

He holds a B.S. in Physics, from the University of New Orleans (2003).

He is a member of Mensa.

He is a husband, and the father of 3 (soon to be 4) lovely children.